AGU PUBLICATIONS

Water Resources Research

RESEARCH ARTICLE
10.1002/2014WR016819

Key Points:
- Analytic approach to compute transient sensitivities using the adjoint method
- Model parameters include distributed transmissivity and storativity
- Parameter fields can be correlated or uncorrelated

Correspondence to:
Z. Lu,
zhiming@lanl.gov

Citation:
Lu, Z., and V. V. Vesselinov (2015), Analytical sensitivity analysis of transient groundwater flow in a bounded model domain using the adjoint method, *Water Resour. Res.*, *51*, 5060–5080, doi:10.1002/2014WR016819.

Received 18 DEC 2014
Accepted 11 JUN 2015
Accepted article online 15 JUN 2015
Published online 3 JUL 2015

Analytical sensitivity analysis of transient groundwater flow in a bounded model domain using the adjoint method

Zhiming Lu[1] and Velimir V. Vesselinov[1]

[1]Computational Earth Science Group (EES-16), MS T003, Los Alamos National Laboratory, Los Alamos, NM 87544, USA

Abstract Sensitivity analyses are an important component of any modeling exercise. We have developed an analytical methodology based on the adjoint method to compute sensitivities of a state variable (hydraulic head) to model parameters (hydraulic conductivity and storage coefficient) for transient groundwater flow in a confined and randomly heterogeneous aquifer under ambient and pumping conditions. For a special case of two-dimensional rectangular domains, these sensitivities are represented in terms of the problem configuration (the domain size, boundary configuration, medium properties, pumping schedules and rates, and observation locations and times), and there is no need to actually solve the adjoint equations. As an example, we present analyses of the obtained solution for typical groundwater flow conditions. Analytical solutions allow us to calculate sensitivities efficiently, which can be useful for model-based analyses such as parameter estimation, data-worth evaluation, and optimal experimental design related to sampling frequency and locations of observation wells. The analytical approach is not limited to groundwater applications but can be extended to any other mathematical problem with similar governing equations and under similar conceptual conditions.

1. Introduction

Sensitivities of state variables to model parameters are computed to perform various types of model analyses [*Saltelli et al.*, 2000]. These include sensitivity analysis, model inversion, parameter estimation, model selection, uncertainty quantification, data-worth analysis, experimental design, and decision analysis. Typically, in these modeling exercises the estimation of sensitivities comprises the dominant part of the computational effort. Furthermore, the accuracy of the modeling analysis is highly dependent on the accuracy of the obtained sensitivity estimates. Therefore, the computational efficiency and the accuracy of the applied methods for sensitivity estimation is of the utmost importance.

Many approaches have been proposed for calculating sensitivities. In the influence coefficient method [*Becker and Yeh*, 1972; *Yeh*, 1986], each parameter is perturbed by a small amount and one forward model run is needed to solve the governing equations using the perturbed parameter value while the rest of parameters are held at their original values; this procedure is repeated for each parameter of interest; the sensitivities are then computed using a finite difference method. The second approach is to solve the sensitivity equation with its corresponding initial and boundary conditions that is derived by differentiating the original governing equation and its initial and boundary conditions with respect to each parameter [*Sykes et al.*, 1985; *Yeh*, 1986]. The sensitivity equation has the same form as the original governing equation. Both methods require a total of $K+1$ forward model runs for a system with K parameters. If the problem is solved using a spatially discretized computational mesh of N grid nodes, and if one is interested in the sensitivity of a state variable (e.g., hydraulic head) to a distributed model parameter (e.g., hydraulic conductivity or storativity) at all grid nodes, one needs to solve governing equations for $N+1$ times. This includes one model run solving for the base case head field in the influence coefficient method or the mean head field in the sensitivity equation method. Furthermore, if the model is transient and solved over a series of M temporal steps, and if one is interested in the sensitivity of a transient state variable at all M steps to a distributed model parameter at all grid nodes N, one needs to solve governing equations for $(M*N)+1$ times. This is not feasible even for a moderately large simulation problem.

Another approach is an analytical sensitivity analysis, in which the groundwater flow problems are solved analytically and sensitivity is then calculated by computing the derivative of the head or drawdown with respect

to transmissivity or storativity. Examples presented in this approach include: sensitivity analysis using the Theis equation [*McElwee and Yukler*, 1978], drawdown sensitivity to the properties of an embedded strip [*Butler and Liu*, 1991] or an embedded disk [*Butler and Liu*, 1993] in an infinite, homogeneous medium. This deterministic approach is limited to some special cases in which an analytical solution of head or drawdown can be obtained, and certainly not feasible for the case with a spatially variable model parameter.

The adjoint method based on the variational approach has been used successfully in a range of fields, such as electrical engineering, meteorology, oceanography, nuclear reactor assessment, hydrogeology, petroleum engineering, and seismology. The adjoint method has been employed to calculate the sensitivity of the head or drawdown to hydraulic parameters (conductivity/transmissivity, storage coefficient/storativity) for steady state flow [*Neuman*, 1980; *Sykes et al*., 1985; *Mazzilli et al*., 2010], transient flow [*Carrera and Medina*, 1994; *Zhu and Yeh*, 2005; *Sun et al*., 2013; *Mao et al*., 2013a], variably saturated flow [*Li and Yeh*, 1998; *Hughson and Yeh*, 1998; *Li and Yeh*, 1999], and multilayer aquifer systems [*Lu et al*., 1988]. Applications of the adjoint method in solute transport include determining the sensitivity of the solute concentration to the source intensity [*Piasecki and Katopodes*, 1997], the contamination source location and travel time probability and distribution [*Neupauer and Wilson*, 1999, 2001; *Larbkich et al*., 2014], and estimates of the historical groundwater contamination distribution [*Michalak and Kitanidis*, 2004]. Other applications of the method in groundwater hydrology include combining the adjoint method with the level set method to identify heterogeneity in porous media [*Lu and Robinson*, 2006] and selection of well locations for minimizing stream depletion [*Neupauer and Cronin*, 2010], among others. There are some recent developments in the method, such as, a multiscale adjoint method for computing high-resolution sensitivity coefficients for subsurface flow in large-scale heterogeneous geologic formations [*Fu et al*., 2010], and the Eulerian-Lagrangian localized adjoint method (ELLAM) for simulating transport in saturated/unsaturated porous media [*Binning and Celia*, 1996; *Ramasomanana et al*., 2012].

Solving the adjoint equation is a computationally efficient way to evaluate parameter sensitivities [*Jacquard et al*., 1965; *Carter et al*., 1974; *Sykes et al*., 1985; *Yeh*, 1986; *Hughson and Yeh*, 1998; *Li and Yeh*, 1998, 1999; *Zhu and Yeh*, 2005; *Leven and Dietrich*, 2006; *Mao et al*., 2013b]. The adjoint equation is derived from the original governing equation and its structure is similar to the original equation. In fact, the adjoint state variable obtained by the solution of the adjoint equation, as seen later, represents the time-reversed head response to a unit pulse source at the observation location and observation time, subject to homogeneous initial and boundary conditions. Therefore, the required computational effort depends on the number of observations, not on the number of parameters. For any problem with M steady state observations, one only needs to solve the governing equation once and the adjoint equation M times. For problems with transient measurements, the adjoint equation needs to be solved backward from the maximum observation time to time zero for each observation location, and therefore, the number of times to solve the adjoint equation is again the number of observation locations. As seen later, this is because, for each observation location, the adjoint state variable at any other observation time can be obtained by simply shifting the solution for the maximum observation time along the time axis, without solving the adjoint equation again. The adjoint state variable is then utilized in evaluating the sensitivity of the state variable to parameters at any location $\mathbf{x}$. This sensitivity is typically presented as an integral over spatial and temporal domains while the integrand is related to the derivatives of the hydraulic head and of the adjoint state variable, and the integral is then evaluated numerically.

In this study, we have developed a novel analytical methodology based on an adjoint method to compute sensitivities of a state variable (hydraulic head) to model parameters (hydraulic conductivity and storage coefficient) in the case of transient groundwater flow in a two-dimensional, spatially correlated or uncorrelated, randomly heterogeneous aquifer under ambient and pumping conditions. One of the major differences between this study and all previous adjoint-based studies on head (or drawdown) sensitivity is that the spatial correlation of the parameter field has been considered, while in previous studies the parameter field is assumed to be uncorrelated and the integral over the entire problem domain was reduced to an exclusive element (or subdomain) containing the point at which the sensitivity is desired [*Neuman*, 1980; *Sun and Yeh*, 1985, 1992; *Yeh*, 1986; *Li and Yeh*, 1998, 1999; *Hughson and Yeh*, 1998; *Zhu and Yeh*, 2005; *Mao et al*., 2013b]. The parameter sensitivities with the adjoint method are typically obtained numerically and the most time-consuming part of the method is on solving the adjoint state equations. In our analytical expressions, these sensitivities are represented directly in terms of the problem configuration (the domain size,

boundary configuration, pumping well locations, pumping schedule and rates), medium properties (the mean and correlation lengths of log transmissivity and log storativity), and observation information (locations and times), and therefore there is no need to solve the adjoint state equations.

The rest of paper is organized as follows. Section 2 gives the statement of the problem. In section 3, the adjoint method is used to derive head sensitivities to transmissivity and storativity; these sensitivities are represented as integrals that are related to the mean flow field and adjoint state variables, which in general need to be evaluated numerically for an arbitrary flow domain. In section 4, we obtain analytical expressions of these sensitivities for spatially uncorrelated or correlated randomly heterogeneous porous media in rectangular domains. Section 5 presents an illustrative example for a typical groundwater flow condition and discusses the effect of the observation location and time on these sensitivities. Section 6 summarizes the conclusions and discusses our future work.

2. Statement of the Problem

We consider transient flow in saturated, two-dimensional, randomly heterogeneous porous media governed by the following equation

$$\nabla \cdot [T(\mathbf{x})\nabla h(\mathbf{x},t)]+\sum_{i=1}^{n_w} Q_i\delta(\mathbf{x}-\mathbf{x}_i^p)I(t_i^s,t_i^e)=S(\mathbf{x})\frac{\partial h(\mathbf{x},t)}{\partial t},\ \mathbf{x}\in\Omega,\ t>0, \tag{1}$$

subject to boundary and initial conditions

$$h(\mathbf{x},t)=H(\mathbf{x}),\ \mathbf{x}\in\Gamma_D,\ t>0, \tag{2}$$

$$-T(\mathbf{x})\nabla h(\mathbf{x},t)\cdot\mathbf{n}=q(\mathbf{x}),\ \mathbf{x}\in\Gamma_N,\ t>0, \tag{3}$$

$$h(\mathbf{x},t)=h_0(\mathbf{x}),\ \mathbf{x}\in\Omega,\ t=0, \tag{4}$$

where $h[m]$ is the hydraulic head, $H[m]$ is the prescribed constant head on the Dirichlet boundary Γ_D, $q[m/s]$ is the prescribed water flux on the Neumann boundary Γ_N, $h_0[m]$ is the initial steady state head in the domain Ω, $T[m^2/s]$ is transmissivity, S is storativity, n_w is the number of pumping or injection wells, $Q_i[m^3/s]$ is the pumping rate (negative for injection) of the i^{th} well located at $\mathbf{x}_i^p=(x_{i1}^p,x_{i2}^p)$, $I(t_i^s,t_i^e)$ is an indicator function (being 1 for $t\in(t_i^s,t_i^e)$ and 0 otherwise), t_i^s is the time pumping starts at the i^{th} well, t_i^e is the time pumping ends at the i^{th} well, δ is the Dirac delta function, $\mathbf{x}=(x_1,x_2)^T$ is the horizontal Cartesian coordinate, $\mathbf{n}$ is the unit vector normal to the boundary of domain $\Gamma=\Gamma_D\cup\Gamma_N$, and t is time.

In a sensitivity analysis, a response function or performance measure can be written as [*Sykes et al.*, 1985; *Zhu and Yeh*, 2005]

$$J(G)=\int_0^{T_e}\int_\Omega G(h,p)d\Omega dt, \tag{5}$$

where Ω represents the spatial domain, T_e is the end of the simulation time, G is an unspecified function of the system state (hydraulic head h), and p is a system parameter (log transmissivity $Y=\ln(T)$ or log storativity $Z=\ln(S)$ in our case).

The marginal sensitivity of the performance J to any parameter p is obtained by taking the derivative of (5) with respect to p:

$$\frac{\partial J}{\partial p}=\int_0^{T_e}\int_\Omega\left(\frac{\partial G(h,p)}{\partial p}+\frac{\partial G(h,p)}{\partial h}\frac{\partial h}{\partial p}\right)d\Omega dt, \tag{6}$$

where the first term represents the explicit dependence of $J(G)$ on parameter p, i.e., the direct effect, while the second term represents the "indirect effect" due to the implicit dependence of $J(G)$ on p through head h. For calculating the sensitivity of hydraulic head to the log transmissivity or log storativity, we choose

$$G=h(\mathbf{x},t)\delta(\mathbf{x}-\mathbf{x}_k)\delta(t-t_l), \tag{7}$$

i.e., the observed head at location $\mathbf{x}_k=(x_{1k},x_{2k})^T$ and time t_l. For this particular function G, $\partial G/\partial p=0$ and $\partial G/\partial h=\delta(\mathbf{x}-\mathbf{x}_k)\delta(t-t_l)$, and (6) reduces to

$$\frac{\partial J}{\partial p}=\int_0^{T_e}\int_\Omega \phi\delta(\mathbf{x}-\mathbf{x}_k)\delta(t-t_l)d\Omega dt, \tag{8}$$

where $\phi=\partial h/\partial p$ is the state sensitivity. Because of the properties of the delta function, this marginal sensitivity in this case is actually $\partial h(\mathbf{x}_k,t_l)/\partial p$, which is to be sought.

3. Solving Sensitivity Using the Adjoint Method

Differentiating (1) with respect to parameter p, which can be either the log transmissivity Y or the log storativity Z,

$$\frac{\partial S}{\partial p}\frac{\partial h}{\partial t}+S\frac{\partial \phi}{\partial t}-\nabla\cdot\left[\frac{\partial T}{\partial p}\nabla h\right]-\nabla\cdot[T\nabla\phi]=0. \tag{9}$$

One may solve for the sensitivity directly from this equation with boundary and initial conditions derived from differentiation of (2)–(4). This is called the direct solution method [*Sykes et al.*, 1985]. However, such a direct solution approach can be computationally very demanding. For example, in a finite element or finite difference computer model with N grid nodes, if one is interested in finding the nodal transmissivity that has the greatest impact on the head at a particular location, one has to solve the above equation N times.

The adjoint method is computationally more efficient [*Neuman*, 1980; *Sykes et al.*, 1985; *Zhu and Yeh*, 2005], requiring evaluations equal to the number of spatial points of interest (typically less than N). Multiplying (9) by an arbitrary differentiable function ϕ^* and integrating over time and space gives

$$\int_0^{T_e}\int_\Omega\left[\frac{\partial S}{\partial p}\frac{\partial h}{\partial t}+S\frac{\partial \phi}{\partial t}-\nabla\cdot\left[\frac{\partial T}{\partial p}\nabla h\right]-\nabla\cdot[T\nabla\phi]\right]\phi^* d\Omega dt=0. \tag{10}$$

Using the partial integration rule on the second term and applying Green's first identity once to the third term and twice to the fourth term, we have

$$\begin{aligned}\int_0^{T_e}\int_\Omega&\left[-S\frac{\partial \phi^*}{\partial t}-\nabla\cdot(T\nabla\phi^*)\right]\phi d\Omega dt+\int_0^{T_e}\int_\Omega\frac{\partial T}{\partial p}\nabla h\cdot\nabla\phi^* d\Omega dt\\&+\int_0^{T_e}\int_\Omega\frac{\partial S}{\partial p}\frac{\partial h}{\partial t}\phi^* d\Omega dt+\int_0^{T_e}\int_{\Gamma_N}\phi T\nabla\phi^*\cdot\mathbf{n}d\Gamma dt\\-\int_0^{T_e}\int_{\Gamma_D}\phi^*&\left[T\nabla\phi+\frac{\partial T}{\partial p}\nabla h\right]\cdot\mathbf{n}d\Gamma dt+\int_\Omega S\phi\phi^*|_{t=Te}d\Omega-\int_\Omega S\phi\phi^*\,|_{t=0}\,d\Omega=0.\end{aligned} \tag{11}$$

In deriving (11) we have used a relationship $(\partial T/\partial p)\nabla h\cdot\mathbf{n}=-\partial q/\partial p-T\nabla\phi\cdot\mathbf{n}=-T\nabla\phi\cdot\mathbf{n}$ on Γ_N, which is derived by differentiating the boundary condition (3).

If we add the terms on the left side of (11) to the right side of (8), the marginal sensitivity becomes

$$\begin{aligned}\frac{\partial J}{\partial p}=&\int_0^{T_e}\int_\Omega\left[\delta(\mathbf{x}-\mathbf{x}_k)\delta(t-t_l)-S\frac{\partial \phi^*}{\partial t}-\nabla\cdot(T\nabla\phi^*)\right]\phi d\Omega dt\\&+\int_0^{T_e}\int_\Omega\frac{\partial T}{\partial p}\nabla h\cdot\nabla\phi^* d\Omega dt+\int_0^{T_e}\int_\Omega\frac{\partial S}{\partial p}\frac{\partial h}{\partial t}\phi^* d\Omega dt\\&+\int_0^{T_e}\int_{\Gamma_N}\phi T\nabla\phi^*\cdot\mathbf{n}d\Gamma dt-\int_0^{T_e}\int_{\Gamma_D}\phi^*\left[T\nabla\phi+\frac{\partial T}{\partial p}\nabla h\right]\cdot\mathbf{n}d\Gamma dt\\&+\int_\Omega S\phi\phi^*|_{t=Te}d\Omega-\int_\Omega S\phi\phi^*\,|_{t=0}\,d\Omega\end{aligned} \tag{12}$$

Because the state sensitivity ϕ is unknown, to evaluate (12), we need to set the coefficient in front of ϕ to be zero (the first term in 12). To simplify (12), we choose the arbitrary function ϕ^* to satisfy the following equation

$$\nabla\cdot[T(\mathbf{x})\nabla\phi^*(\mathbf{x},t)]-\delta(\mathbf{x}-\mathbf{x}_k)\delta(t-t_l)=-S(\mathbf{x})\frac{\partial\phi^*(\mathbf{x},t)}{\partial t},\ \mathbf{x}\in\Omega,\ t>0 \tag{13}$$

with boundary and terminal conditions

$$\phi^*(\mathbf{x},t)=0,\ \mathbf{x}\in\Gamma_D,\ t>0, \tag{14}$$

$$-T\nabla\phi^*(\mathbf{x},t)\cdot\mathbf{n}=0,\ \mathbf{x}\in\Gamma_N,\ t>0, \tag{15}$$

$$\phi^*(\mathbf{x},t)=0,\ \mathbf{x}\in\Omega,\ t=T_e, \tag{16}$$

which reduces the marginal sensitivity (12) to

$$\frac{\partial J}{\partial p}=\int_0^{T_e}\int_\Omega\frac{\partial T}{\partial p}\nabla h\cdot\nabla\phi^* d\Omega dt+\int_0^{T_e}\int_\Omega\frac{\partial S}{\partial p}\frac{\partial h}{\partial t}\phi^* d\Omega dt-\int_\Omega S\phi\phi^*|_{t=0}\,d\Omega. \tag{17}$$

Equation (13) with conditions (14)–(16) is called the adjoint equation. Note that the adjoint equation and its associated boundary and initial conditions are independent of any pumping/injection wells and prescribed boundary conditions in the original flow model (1)–(4). In other words, if one adds more wells or changes the constant head or fluxes at the boundary, there is no need to solve the adjoint equation again (as long as the boundary types remain the same). This is one of the advantages of the adjoint method. We also note that the initial-boundary value problem given by (13)–(16) is the backward flow equation, and in order for it to have a unique solution, we must prescribe a terminal condition at $t=T_e$ instead of at $t=0$.

In some studies [*Zhu and Yeh*, 2005; *Mao et al*., 2013b; *Sun et al*., 2013], the initial head field $h_0(\mathbf{x})$ is assumed to be independent of the transmissivity field and the last term in (17) was dropped. However, the initial head generally depends on the transmissivity field and therefore $\phi=\partial h/\partial p$ is nonzero at $t=0$ when the parameter of concern is transmissivity, and the last term in (17) cannot be dropped. It should be emphasized that knowing the initial head distribution a priori does not mean $\phi=\partial h/\partial Y$ is zero at time zero [*Zhu and Yeh*, 2005], unless the initial head is independent of transmissivity, such as the case with hydrostatic initial head [*Li and Yeh*, 1998]. In section 5, we will investigate through numerical examples the contribution of this term to the total sensitivity. To evaluate this term, following *Hughson and Yeh* [1998] and *Li and Yeh* [1999], we assume that the initial head satisfies the steady state flow equation

$$\nabla\cdot[T(\mathbf{x})\nabla h_0(\mathbf{x})]=0, \tag{18}$$

subject to the same boundary conditions as for the transient flow: $h_0(\mathbf{x})=H(\mathbf{x})$ for $\mathbf{x}\in\Gamma_D$, and $-T(\mathbf{x})\nabla h_0(\mathbf{x})\cdot\mathbf{n}=q(\mathbf{x})$ for $\mathbf{x}\in\Gamma_N$. Following the same procedure as we did for the transient flow, i.e., taking the derivative of (18) with respect to Y, multiplying the resulting equation by an arbitrary function ϕ_0^*, integrating it over domain Ω, and applying Green's first identity, yields

$$\int_\Omega\phi_0\nabla\cdot(T\nabla\phi_0^*)d\Omega-\int_\Omega\frac{\partial T}{\partial Y}\nabla h_0\cdot\nabla\phi_0^* d\Omega-\int_{\Gamma_N}\phi_0 T\nabla\phi_0^*\cdot\mathbf{n}d\Gamma-\int_{\Gamma_D}\frac{\partial q}{\partial Y}\phi_0^* d\Gamma=0, \tag{19}$$

where $\phi_0=\partial h_0/\partial Y$. Note that, in deriving the last two terms in the above equation, we have used the fact that $\phi_0\equiv 0$ on Γ_D and $\partial q/\partial Y\equiv 0$ on Γ_N. By adding (19) to (17) and choosing ϕ_0^* satisfying

$$\nabla\cdot\left[T(\mathbf{x})\nabla\phi_0^*(\mathbf{x})\right]+S\phi^*(\mathbf{x},0)=0, \tag{20}$$

subject to the following boundary conditions

$$\phi_0^*(\mathbf{x})=0,\ \mathbf{x}\in\Gamma_D, \tag{21}$$

$$-T\nabla\phi_0^*(\mathbf{x})\cdot\mathbf{n}=0,\ \mathbf{x}\in\Gamma_N, \tag{22}$$

the marginal sensitivity (17) becomes

$$\frac{\partial J}{\partial p}=\int_0^{T_e}\int_\Omega\frac{\partial T}{\partial p}\nabla h\cdot\nabla\phi^* d\Omega dt+\int_0^{T_e}\int_\Omega\frac{\partial S}{\partial p}\frac{\partial h}{\partial t}\phi^* d\Omega dt+\int_\Omega\frac{\partial T}{\partial Y}\nabla h_0\cdot\nabla\phi_0^* d\Omega, \tag{23}$$

where the last term is applicable only if the parameter p is the log transmissivity.

We should mention that there is some confusion in the literature on the form of the adjoint equation and sensitivity expressions [*Zhu and Yeh*, 2005; *Mao et al*., 2013b; *Sun et al*., 2013]. If we had added the terms on

the left side of (11) to the left side of (6), we would have derived a slightly different adjoint equation than the one presented in (13), and the sign in front of the second term of (13) would be positive. In this case, all terms in (23) would be negative. Either way, there must be a negative sign in front of the right side of (13), unless the adjoint equation and its terminal condition are written in terms of the reverse of the time ($\tau = t_l - t$), as in *Yeh* [1986] and *Leven and Dietrich* [2006]. In the latter case, the adjoint state variable $\phi^*(\mathbf{x}, t)$ in (23) should be replaced by $\phi^*(\mathbf{x}, t_l - t)$.

Once h, h_0, ϕ^*, and ϕ_0^* are obtained, the sensitivity of the head at location $\mathbf{x}_k$ at time t_l to the log transmissivity Y or log storativity Z at any point $\mathbf{x} = (x_1, x_2)^T \in \Omega$ can be obtained from (23) by replacing parameter p by $Y = \ln(T)$ or $S = \ln(S)$. If we assume that Y and Z are uncorrelated, then

$$y^{(k,l)}(\mathbf{x}) \triangleq \frac{\partial h(\mathbf{x}_k, t_l)}{\partial Y(\mathbf{x})} = \int_0^{T_e} \int_\Omega \frac{\partial T(\chi)}{\partial Y(\mathbf{x})} \nabla h(\chi, t) \cdot \nabla \phi(\chi, t) d\chi dt + \int_\Omega \frac{\partial T(\chi)}{\partial Y(\mathbf{x})} \nabla h_0(\chi) \cdot \nabla \phi_0^*(\chi) d\chi, \tag{24}$$

and

$$z^{(k,l)}(\mathbf{x}) \triangleq \frac{\partial h(\mathbf{x}_k, t_l)}{\partial Z(\mathbf{x})} = \int_0^{T_e} \int_\Omega \frac{\partial S(\chi)}{\partial Z(\mathbf{x})} \frac{\partial h(\chi, t)}{\partial t} \phi(\chi, t) d\chi dt, \tag{25}$$

where $y^{(k,l)}(\mathbf{x})$ and $z^{(k,l)}(\mathbf{x})$ are defined for convenience, and $d\Omega$ has been replaced by $d\chi$ to avoid confusion. These sensitivity values represent the infinitesimal rate of change in hydraulic head at the given measurement location $\mathbf{x}_k$ and time t_l, due to an infinitesimal change of log transmissivity or log storativity.

The procedure for finding transient state sensitivities can be summarized as follows. For any given transmissivity field, one first solves for h_0 from the steady state flow equation (18) with appropriate boundary conditions. With this initial condition, one then solves for the transient head h from (1) with boundary and initial conditions (2)–(4). The state variable ϕ^* is obtained from the backward solution of (13) with boundary and terminal conditions (14)–(16). The solution at time zero $\phi^*(\mathbf{x}, 0)$ is then used as a source in solving ϕ_0^* from (20) with boundary conditions (21)–(22). Finally, the state sensitivities are evaluated from (24) and (25).

If one is interested in sensitivities of the steady state head to log transmissivity, one can follow the same procedure described above for the transient flow and derive the marginal sensitivity as

$$\frac{\partial J}{\partial Y} = \int_\Omega \frac{\partial T}{\partial Y} \nabla h_{ss} \cdot \nabla \phi_{ss}^* d\Omega, \tag{26}$$

and the head sensitivity to log transmissivity can be written as

$$y_{ss}^{(k)}(\mathbf{x}) \triangleq \frac{\partial h_{ss}(\mathbf{x}_k)}{\partial Y(\mathbf{x})} = \int_\Omega \frac{\partial T(\chi)}{\partial Y(\mathbf{x})} \nabla h_{ss}(\chi) \cdot \nabla \phi_{ss}^*(\chi) d\chi, \tag{27}$$

where ϕ_{ss}^* is the adjoint state variable for the steady state flow, obtained from the following equation

$$\nabla \cdot \left[T(\mathbf{x}) \nabla \phi_{ss}^*(\mathbf{x}) \right] - \delta(\mathbf{x} - \mathbf{x}_k) = 0, \ \mathbf{x} \in \Omega, \tag{28}$$

with boundary conditions $\phi_{ss}^*(\mathbf{x}) = 0$ for $\mathbf{x} \in \Gamma_D$, and $T \nabla \phi_{ss}^*(\mathbf{x}) \cdot \mathbf{n} = 0$ for $\mathbf{x} \in \Gamma_N$. Note that for steady state flow, storativity is not relevant and therefore the head sensitivity to the log storativity is zero.

We should emphasize that the sensitivity $\partial h / \partial p$ can be evaluated for any given transmissivity and/or storativity field. However, in many practical problems (such as inverse problems), the true transmissivity/storativity fields are unknown, and therefore h, h_0, ϕ^*, and ϕ_0^* are typically evaluated at the mean transmissivity/storativity fields [*Sun and Yeh*, 1985, 1992; *Zhu and Yeh*, 2005].

4. Sensitivity for Rectangular Domains

In general, h, h_0, ϕ^*, and ϕ_0^* have to be evaluated numerically. In this paper, we consider a special case in which the domain Ω is a rectangle of size $L_1 \times L_2$, and the boundary and initial conditions are given as

$$h(\mathbf{x},t)=H_1,\ x_1=0,\ t>0, \tag{29}$$

$$h(\mathbf{x},t)=H_2,\ x_1=L_1,\ t>0, \tag{30}$$

$$\partial h(\mathbf{x},t)/\partial x_2=0,\ \ x_2=0,\ t>0, \tag{31}$$

$$\partial h(\mathbf{x},t)/\partial x_2=0,\ \ x_2=L_2,\ t>0, \tag{32}$$

$$h(\mathbf{x},t)=h_0(\mathbf{x}),\ \mathbf{x}\in\Omega,\ t=0. \tag{33}$$

For simplicity, we further assume $h_0=H_1+(H_2-H_1)x_1/L_1$.

4.1. Solving for the Mean Head

At the first order, the governing equation for the mean head can be derived by replacing T and S in (1) with their mean counterparts $\bar{T}$ and $\bar{S}$ [*Sun and Yeh*, 1985, 1992; *Zhu and Yeh*, 2005]

$$\nabla\cdot\left[\bar{T}\nabla\bar{h}(\mathbf{x},t)\right]+\sum_{i=1}^{n_w}Q_i\delta(\mathbf{x}-\mathbf{x}_i^p)I(t_i^s,t_i^e)=\bar{S}\frac{\partial\bar{h}(\mathbf{x},t)}{\partial t},\ \mathbf{x}\in\Omega,\ t>0. \tag{34}$$

Under the given boundary and initial conditions (29)–(33), following the techniques presented in *Özişik* [1989] and *Lu and Zhang* [2003, 2005], the solution can be written as

$$\bar{h}(\mathbf{x},t)=h_0(\mathbf{x})+\frac{4}{D\bar{T}}\sum_{\substack{m=1\\n=0}}^{\infty}\frac{a_n}{\omega_{mn}^2}\sin(\alpha_m x_1)\cos(\beta_n x_2)\sum_{i=1}^{n_w}p_{mn}^{(i)}w_{mn}^{(i)}(t), \tag{35}$$

where $p_{mn}^{(i)}=Q_i\sin(\alpha_m x_{i1}^p)\cos(\beta_n x_{i2}^p)$, $\omega_{mn}^2=\alpha_m^2+\beta_n^2$, $\alpha_m=m\pi/L_1$, $m=1,2,\cdots$, $\beta_n=n\pi/L_2$, $n=0,1,2,\cdots$, $D=L_1L_2$, $a_n=1$ for $n\geq 1$ and $a_n=1/2$ for $n=0$, and

$$w_{mn}^{(i)}(t)=\begin{cases}0 & \text{if } t<t_i^s\\ 1-e^{-\frac{\bar{T}}{S}\omega_{mn}^2(t-t_i^s)} & \text{if } t_i^s<t<t_i^e\\ e^{-\frac{\bar{T}}{S}\omega_{mn}^2(t-t_i^e)}-e^{-\frac{\bar{T}}{S}\omega_{mn}^2(t-t_i^s)} & \text{if } t>t_i^e\end{cases}. \tag{36}$$

The last term in (35) represents the head drawdown due to pumping. Equations (35) and (36) were derived for the case with a single pumping period at each well. However, by the superposition principle, the equations are also applicable to the case for wells with an arbitrary number of pumping periods with constant pumping rates. In fact, for any well with multiple pumping periods, we can simply treat the well as multiple wells, each of which has a single period with a constant pumping rate. In this sense, the summation over all pumping wells in (35) is actually a summation over all pumping periods.

4.2. Solving the Adjoint State Equations

For the adjoint state equation (13), the boundary and terminal conditions corresponding to boundary and initial conditions for the simplified (rectangular) model domain (29)–(33) are

$$\phi^*(\mathbf{x},t)=0,\ x_1=0,L_1;\ t>0, \tag{37}$$

$$\partial\phi^*(\mathbf{x},t)/\partial x_2=0,\ \ x_2=0,L_2;\ t>0, \tag{38}$$

$$\phi^*(\mathbf{x},t)=0,\ \mathbf{x}\in\Omega,\ t=T_e. \tag{39}$$

By simply changing the variable $t=T_e-\tau$, (13) with boundary conditions (37) and (38) and terminal condition (39) can be modified to a set of similar equations in terms of τ with an initial condition. The final solution can be expressed as

$$\phi^*(\mathbf{x},t)=-\frac{4}{\bar{S}D}\sum_{\substack{m=1\\n=0}}^{\infty}a_n\sin(\alpha_m x_1)\cos(\beta_n x_2)O_{mn}^k e^{-\frac{\bar{T}}{S}\omega_{mn}^2(t_l-t)},\ \text{for } t\leq t_l, \tag{40}$$

and $\phi^*(\mathbf{x},t)=0$ for $t>t_l$. Here $O_{mn}^k=\sin(\alpha_m x_{1k})\cos(\beta_n x_{2k})$, and $\mathbf{x}_k=(x_{1k},x_{2k})^T$ are the observation locations. It is seen from (40) that, for a fixed observation location $\mathbf{x}_k$ and t_l, the adjoint state function $\phi^*(\mathbf{x},t)$ depends on the time difference t_l-t. An important implication is that, for a given observation location $\mathbf{x}_k$, one may

solve for the state variable, denoted as $\phi^*_{km}(\mathbf{x},t)$ for clarification, using the maximum observation time at this location, say, t_m. Then for any observation time $t_n < t_m$, there is no need to solve the adjoint state equation again because $\phi^*_{kn}(\mathbf{x},t)=\phi^*_{km}(\mathbf{x},t_m-t_n+t)$. In other words, the adjoint state variable at any time can be derived by simply shifting the state variable for the maximum observation time along the time axis, without solving the adjoint equation again. This result is consistent with observation of *Carrera and Medina* [1994] and *Mao et al.* [2013b].

It is noted that $\phi^*(\mathbf{x},t)$ represents the backward head response to instantaneous pumping at location $\mathbf{x}_k$ at time t_l under homogeneous initial and boundary conditions. It is clear that $\phi^*(\mathbf{x},t)$ is zero everywhere for time $t \in (t_l, T_e)$ and it reaches its maximum at $t=t_l^-$ due to instantaneous unit pumping at t_l. As time goes from t_l to zero, $\phi^*(\mathbf{x},t)$ decreases. It should also be noted that although it is solved backward from $t = T_e$, the adjoint state is independent of the terminal time T_e. In practice, as said previously, we may simply choose T_e as the maximum observation time t_l for convenience. In the sequel, t_l rather than T_e is used.

Once $\phi^*(\mathbf{x},t)$ is evaluated, the adjoint state variable ϕ^*_0 is obtained from solving (20) with a source term $\phi^*(\mathbf{x},0)$ and homogeneous boundary conditions $\phi^*_0(\mathbf{x})=0$ at $x_1=0$ and $x_1 = L_1$, and $\partial\phi^*_0(\mathbf{x})/\partial x_2=0$ at $x_2=0$ and $x_2 = L_2$. The solution is

$$\phi^*_0(\mathbf{x})=-\frac{4}{\bar{T}D}\sum_{\substack{m=1\\n=0}}^{\infty}\frac{a_n O^k_{mn}}{\omega^2_{mn}}\sin(\alpha_m x_1)\cos(\beta_n x_2)e^{-\frac{\bar{T}}{\bar{S}}\omega^2_{mn}t_l}. \tag{41}$$

This solution indicates that, for sufficiently large observation time t_l, ϕ^*_0 approaches zero and the third term in (23) may be dropped. Note that this is different from the adjoint state variable ϕ^*_{ss} that corresponds to the steady state flow, which is obtained from (28)

$$\phi^*_{ss}(\mathbf{x})=-\frac{4}{\bar{T}D}\sum_{\substack{m=1\\n=0}}^{\infty}\frac{a_n O^k_{mn}}{\omega^2_{mn}}\sin(\alpha_m x_1)\cos(\beta_n x_2). \tag{42}$$

This can be used in calculating steady state head sensitivity using (27).

4.3. Sensitivities for Uncorrelated Fields

The expressions for state sensitivities (24), (25), and (27) indicate that these sensitivities depend on the auto-correlation of the log transmissivity or log storativity fields.

4.3.1. Head Sensitivity to Log Transmissivity

By noting

$$\frac{\partial T(\chi)}{\partial Y(\mathbf{x})}=\frac{\partial T(\chi)}{\partial Y(\chi)}\frac{\partial Y(\chi)}{\partial Y(\mathbf{x})}=T(\chi)\frac{\partial Y(\chi)}{\partial Y(\mathbf{x})},$$

Equation (24) can be rewritten as

$$y^{(k,l)}(\mathbf{x})=\int_0^{t_l}\int_\Omega T(\chi)\frac{\partial Y(\chi)}{\partial Y(\mathbf{x})}\nabla\phi^*\cdot\nabla\bar{h}\,d\chi dt+\int_\Omega T(\chi)\frac{\partial Y(\chi)}{\partial Y(\mathbf{x})}\nabla\phi^*_0\cdot\nabla h_0\,d\chi. \tag{43}$$

The spatial integration is over the entire domain Ω and the sensitivity depends on the spatial correlation of the transmissivity field. In the literature, it is typically assumed that $Y(\chi)$ is independent of $Y(\mathbf{x})$ for $\mathbf{x}\neq\chi$, and this expression is further reduced to

$$y^{(k,l)}(\mathbf{x})=\bar{T}\int_0^{t_l}\int_{\Omega_e(\mathbf{x})}\nabla\phi^*(\chi,t)\cdot\nabla\bar{h}(\chi,t)d\chi dt+\bar{T}\int_{\Omega_e(\mathbf{x})}\nabla\phi^*_0(\chi)\cdot\nabla h_0(\chi)d\chi, \tag{44}$$

where $\Omega_e(\mathbf{x})$ is the computational grid element containing the point $\mathbf{x}$ [*Neuman*, 1980; *Sun and Yeh*, 1985, 1992; *Yeh*, 1986; *Li and Yeh*, 1998, 1999; *Hughson and Yeh*, 1998; *Zhu and Yeh*, 2005; *Mao et al.*, 2013b]. In a uniformly discretized numerical mesh of rectangular elements of size $\Delta x_1\times\Delta x_2$, $\Omega_e(\mathbf{x})$ represents an element centered at $\mathbf{x}$. Note that T and h in (43) have been replaced by their mean quantities $\bar{T}$ and $\bar{S}$, and $\bar{h}$ is the mean head field obtained from the solution of (1)–(4) using $\bar{T}$ and $\bar{S}$. The sensitivity of head at observation location $\mathbf{x}_k$ at time t_l with respect to log transmissivity $Y(\mathbf{x})$ can be derived by taking derivatives of (35) and (40), substituting these derivatives into (44), and integrating over the temporal and spatial domains:

$$y^{(k,l)}(\mathbf{x}) = \frac{4J_0}{D}\sum_{\substack{m=1\\n=0}}^{\infty}\frac{a_n\alpha_m}{\omega_{mn}^2}u_1(\alpha_m)u_2(\beta_n)O_{mn}^k - \frac{16}{D^2\bar{T}}\sum_{\substack{m,m_1=1\\n,n_1=0}}^{\infty}\frac{a_n a_{n_1}}{\omega_{mn}^2}\left[\alpha_m\alpha_{m_1}F_1^+(\alpha_m,\alpha_{m_1})F_2^+(\beta_n,\beta_{n_1}) + \beta_n\beta_{n_1}F_1^-(\alpha_m,\alpha_{m_1})F_2^-(\beta_n,\beta_{n_1})\right]O_{m_1n_1}^k\sum_{i=1}^{n_w}p_{mn}^{(i)}I_T^{(i)}, \tag{45}$$

where $J_0=(H_1-H_2)/L_1$ is the initial steady state hydraulic gradient, $p_{mn}^{(i)}=Q_i\sin(\alpha_m x_{i1}^p)\cos(\beta_n x_{i2}^p)$, and the definitions of functions u_1, u_2, F_1^+, F_1^-, F_2^+, F_2^-, and $I_T^{(i)}$ are given in Appendix A.

The first term in (45) represents the head sensitivity due to the initial steady state head, while the second term accounts for the contribution from pumping. As we mentioned previously, the effect of the initial head to total head sensitivity vanishes if the head distribution is independent of the transmissivity, as in our case, when the initial head $h_0(\mathbf{x})=H_1-J_0x_1$. This initial head distribution implies the assumption that the transmissivity field is uniform over the entire domain. If we substitute ϕ_{ss} and $h_{ss}=h_0$ into (27) and carry out the integration, we find that the steady state head sensitivity $y_{ss}^{(k)}(\mathbf{x})$ is exactly the same as the first term in (45), which should be zero for this initial head. The presence of the first term is due to the assumption of an uncorrelated transmissivity field (i.e., using exclusive element Ω_e) rather than a uniform transmissivity field. In an extreme case where Ω_e is taken to be the entire domain, this term is zero, as expected. In fact, if we choose $(x_1,x_2)=(L_1/2,L_2/2)$, i.e., the central point, and $\Delta x_1=L_1$ and $\Delta x_2=L_2$, both $u_1(\alpha_m)$ and $u_2(\beta_n)$ are zero (see expressions in Appendix A), and the first term vanishes.

We should emphasize that the final head sensitivity shown in (45) is represented directly in terms of the problem configuration (the domain size, boundary configuration, pumping well locations, pumping schedule and rates), medium properties (the mean and correlation lengths of log transmissivity and log storativity), and observation information (locations and times). It is not needed to solve the adjoint state equations.

The sensitivity defined in (44) or (45) depends on the size of the grid element. Because the domain discretization is not relevant for analytical solutions, it is natural to normalize the sensitivity by the area of the element $\Omega_e(\mathbf{x})$, which is $\Delta x_1\Delta x_2$ for rectangular elements. From (45) it is seen that the sensitivity is a nonlinear function of $\Delta x_1\Delta x_2$, and thus the normalized sensitivity is still dependent on the size of the element. We consider a limiting case where the size of the element approaches zero, and the head sensitivity can be written as

$$y^{(k,l)}(\mathbf{x}) = \frac{4J_0}{D}\sum_{\substack{m=1\\n=0}}^{\infty}\frac{a_n\alpha_m}{\omega_{mn}^2}\cos(\alpha_m x_1)\cos(\beta_n x_2)O_{mn}^k - \frac{16}{D^2\bar{T}}\sum_{\substack{m,m_1=1\\n,n_1=0}}^{\infty}\frac{a_n a_{n_1}}{\omega_{mn}^2}\left[\alpha_m\alpha_{m_1}C_4+\beta_n\beta_{n_1}S_4\right]O_{m_1n_1}\sum_{i=1}^{n_w}p_{mn}^{(i)}I^{(i)}, \tag{46}$$

where

$$C_4=\cos(\alpha_m x_1)\cos(\alpha_{m_1}x_1)\cos(\beta_n x_2)\cos(\beta_{n_1}x_2),$$
$$S_4=\sin(\alpha_m x_1)\sin(\alpha_{m_1}x_1)\sin(\beta_n x_2)\sin(\beta_{n_1}x_2).$$

These equations may also be derived directly from (44) by first letting $\Omega_e(\mathbf{x})$ approach the point $\mathbf{x}$ and then carrying the integration over the time domain.

It is of interest to investigate the contribution of the last term in (23) or (24), denoted as $y_1^{(k,l)}(\mathbf{x})$, which is related to the dependence of the initial head to the transmissivity field and is ignored in some previous studies [cf. *Mao et al.*, 2013b].

$$y_1^{(k,l)}(\mathbf{x}) = \frac{4J_0}{D}\sum_{\substack{m=1\\n=0}}^{\infty}\frac{a_n\alpha_m}{\omega_{mn}^2}u_1(\alpha_m)u_2(\beta_n)O_{mn}^k e^{-\frac{\bar{T}}{S}\omega_{mn}^2 t_l}, \tag{47}$$

which again is nonzero for any exclusive element smaller than the domain. This term depends on the observation time and it cancels out the other term (with an opposite sign) resulting from the first integral in (23)

or (24). Therefore, neglecting the last term in (23) or (24) will result in a unrealistic scenario in which the sensitivity is time-dependent even if there is no pumping/injection and the head becomes steady state.

4.3.2. Head Sensitivity to Log Storativity

Similarly, from (25), we have

$$z^{(k,l)}(\mathbf{x}) = \bar{S}\int_0^{t_l}\int_\Omega \frac{\partial \bar{h}(\chi,t)}{\partial t}\phi^*(\chi,t)d\chi dt. \tag{48}$$

Substituting $\bar{h}$ and ϕ^* into this equation yields

$$z^{(k,l)}(\mathbf{x}) = -\frac{16}{D^2\bar{T}}\sum_{\substack{m,m_1=1\\ n,n_1=0}}^{\infty} a_n a_{n_1} F_1^-(\alpha_m,\alpha_{m_1})F_2^+(\beta_n,\beta_{n_1})O^k_{m_1 n_1}\sum_{i=1}^{n_w} p^{(i)}_{mn} I_S^{(i)} \tag{49}$$

where F_1^-, F_2^+, and $I_S^{(i)}$ are given in Appendix A. As the size of the element approaches zero, i.e., $\Omega_e(\mathbf{x}) \to \mathbf{x}$, (49) becomes

$$z^{(k,l)}(\mathbf{x}) = -\frac{16}{D^2\bar{T}}\sum_{\substack{m,m_1=1\\ n,n_1=0}}^{\infty} a_n a_{n_1} Sc\, O^k_{m_1 n_1}\sum_{i=1}^{n_w} p^{(i)}_{mn} I_S^{(i)}, \tag{50}$$

where $Sc = \sin(\alpha_m x_1)\sin(\alpha_{m1}x_1)\cos(\beta_n x_2)\cos(\beta_{n1}x_2)$. Note that this sensitivity is independent of the initial flow field.

4.4. Sensitivities for Correlated Fields

4.4.1. Head Sensitivity to Log Conductivity

For a correlated transmissivity field, one first needs to derive the relationship between $Y(\chi)$ and $Y(\mathbf{x})$. Consider the conditional mean field $Y(\chi)$ due to a single conditioning point $\mathbf{x}$. Using the simple kriging expression, we have

$$Y(\chi) = \langle Y(\chi)\rangle + \frac{C_Y(\mathbf{x},\chi)}{C_Y(\mathbf{x},\mathbf{x})}[Y(\mathbf{x}) - \langle Y(\mathbf{x})\rangle]. \tag{51}$$

where $C_Y(\mathbf{x},\chi)$ is the covariance function of the log transmissivity at locations $\mathbf{x} = (x_1,x_2)^T$, $\chi = (\chi_1,\chi_2)^T$, and $\langle Y(\chi)\rangle$ is the unconditional mean field. The unconditional mean field is a constant for a statistically homogeneous field. If the covariance function is written as $C_Y(\mathbf{x},\chi) = \sigma_Y^2\rho_Y(|\mathbf{x}-\chi|)$, where ρ_Y is a correlation function, from (51), we have

$$\frac{\partial Y(\chi)}{\partial Y(\mathbf{x})} = \frac{C_Y(\mathbf{x},\chi)}{C_Y(\mathbf{x},\mathbf{x})} = \rho_Y(|\mathbf{x}-\chi|). \tag{52}$$

For a separable exponential correlation function $\rho_Y(\mathbf{x},\chi) = \sigma_Y^2\exp(-|x_1-\chi_1|/\lambda_{Y,1} - |x_2-\chi_2|/\lambda_{Y,2})$, where $\lambda_{Y,1}$ and $\lambda_{Y,2}$ are the correlation lengths of Y in x_1 and x_2 directions, respectively, substituting this into (43) yields

$$y^{(k,l)}(\mathbf{x}) = \bar{T}\int_0^{t_l}\int_\Omega e^{-\frac{|x_1-\chi_1|}{\lambda_{Y,1}} - \frac{|x_2-\chi_2|}{\lambda_{Y,2}}}\nabla\phi^*(\chi,t)\cdot\nabla\bar{h}(\chi,t)d\chi dt. \tag{53}$$

Carrying out the integrations results an expression with the same structure as in (45) except that the functions u_1, u_2, $F_1^\pm$, $F_2^\pm$ need to be redefined as shown in Appendix B.

4.4.2. Head Sensitivity to Log Storativity

Similarly, we can write the relationship $\partial Z(\chi)/\partial Z(\mathbf{x}) = \rho_Z(\mathbf{x},\chi)$. From (25), we have

$$z^{(k,l)}(\mathbf{x}) = \bar{S}\int_0^{t_l}\int_\Omega e^{-\frac{|x_1-\chi_1|}{\lambda_{Z,1}} - \frac{|x_2-\chi_2|}{\lambda_{Z,2}}}\frac{\partial \bar{h}(\chi,t)}{\partial t}\phi^*(\chi,t)d\chi dt. \tag{54}$$

Substituting the expressions of $\bar{h}$ and ϕ^* into this equation and carrying out the integration yields an expression with the same format as (49) except that functions F_1^- and F_2^+ need to be redefined, as shown in Appendix B. It should be noted that there is no restriction on the type of the covariance function C_Y. Using the separable exponential covariance allows us to derive these sensitivities analytically.

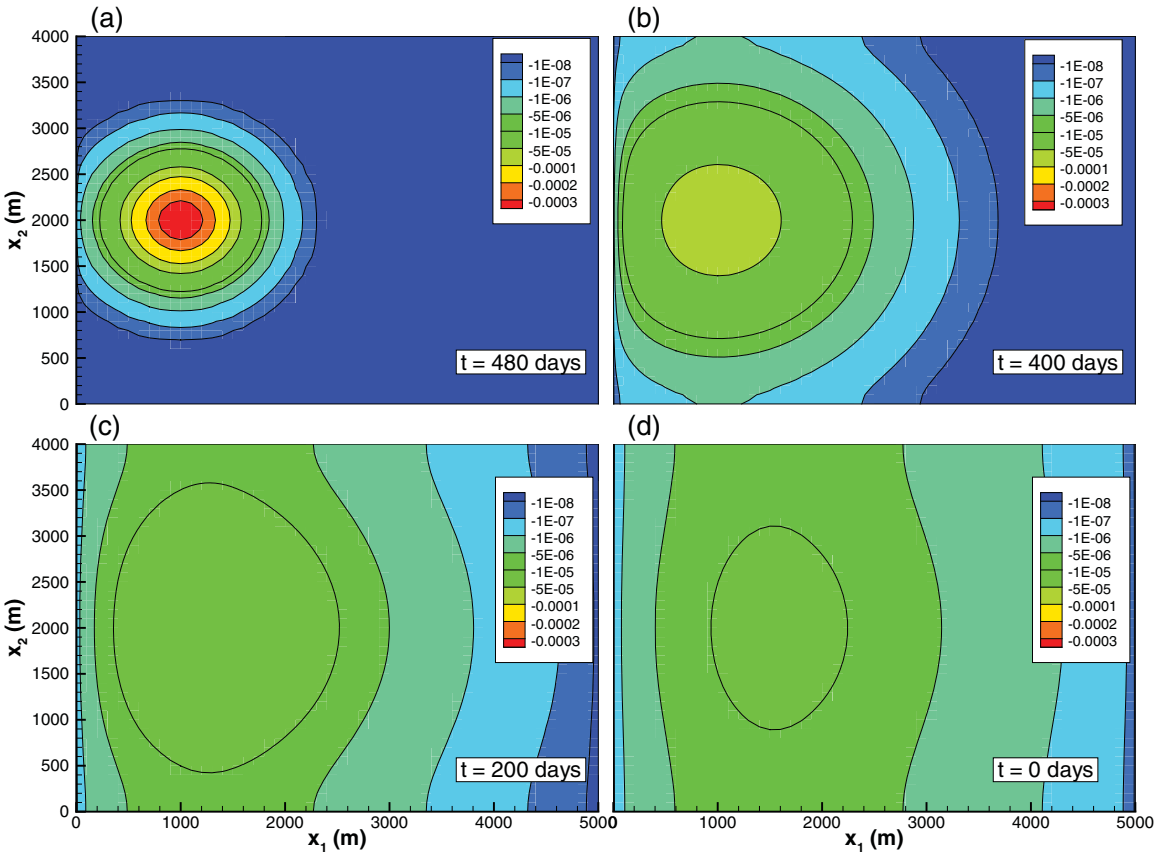

Figure 1. Contour maps of the adjoint state variable $\phi^*(\mathbf{x}, t)$ associated with head observation at well $\mathbf{x}_k = (1000\,\text{m}, 2000\,\text{m})$ at $t_l = 500$ days for various times before the time of observation t_l.

5. Numerical Examples

To illustrate the analytical solutions, we consider a two-dimensional rectangular domain of size $L_1 = 5000$ m and $L_2 = 4000$ m (Figure 1). The boundary conditions are: constant heads $H_1 = 1001$ m and $H_2 = 1000$ m on the left and right boundaries, and no-flow on two lateral boundaries. Hydraulic parameters include a mean transmissivity of $\bar{T} = 10\,\text{m}^2/\text{d}$ and mean storativity of $\bar{S} = 0.005$. These parameter fields can be either uncorrelated (with the correlation scale less than the size of elements in the numerical mesh) or correlated. For the case of correlated fields, the correlation lengths for both log transmissivity and log storativity are assumed to be the same but may be anisotropic: $\lambda_{Y,1} = \lambda_{Z,1} = 250$ m and $\lambda_{Y,2} = \lambda_{Z,2} = 200$ m. We consider two flow scenarios, one without pumping (Case A) and the other with constant pumping (Case B) at the center of the model domain, $\mathbf{x}_1^p = (2500\,\text{m}, 2000\,\text{m})^T$ and at a pumping rate of $Q_1 = 20\,\text{m}^3/\text{d}$. A single observation well is placed at $\mathbf{x}_k = (1000\,\text{m}, 2000\,\text{m})$, except for cases in which various observation locations are used to explore the effect of the observation location on the sensitivity coefficients.

5.1. Adjoint State Variables

We first explore some features of the adjoint state variables $\phi^*(\mathbf{x}, t)$ and $\phi_0^*(\mathbf{x})$, both of which are independent of pumping/injection within the domain and the actual values specified on flow boundaries. These adjoint state variables, though not explicitly denoted, are functions of observation location $\mathbf{x}_k$ and time t_l. Figure 1 illustrates the adjoint state variable $\phi^*(\mathbf{x}, t)$ associated with the head observed at $\mathbf{x}_k$ at time $t_l = 500$ days at various elapsed times. Because the solving for the adjoint state variable is equivalent to solving for the head (in reversed time) with an instantaneous unit pumping at location $\mathbf{x}_k$ at time t_l under the homogeneous terminal and boundary conditions, it has a maximum peak at time t_l and then its magnitude decreases with an increasing zone of "influence" (area with nonzero adjoint-state values) as time goes from t_l to zero (Figure 1d). The solution at time zero, $\phi^*(\mathbf{x}, 0)$, is then used as a source function in solving for the adjoint state variable $\phi_0^*(\mathbf{x})$, shown in Figure 2, which depicts $\phi_0^*(\mathbf{x})$ for two observation times $t_l = 1$

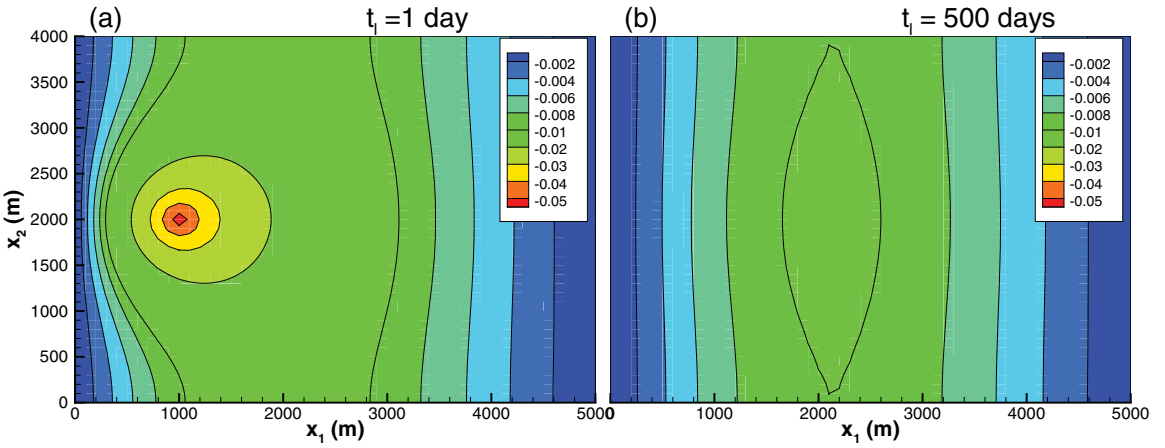

Figure 2. Contour maps of the adjoint state variable $\phi_0^*(\mathbf{x})$ associated head observation at at well $\mathbf{x}_k = (1000\,\text{m}, 2000\,\text{m})$ at (a) 1 day and (b) 500 days.

day and $t_l = 500$ days. It should be noted that, although $\phi_0^*(\mathbf{x})$ is independent of time, it does depend on $\mathbf{x}_k$ and t_l through the source function $\phi^*(\mathbf{x}, 0)$, which is a function of $\mathbf{x}_k$ and t_l.

Because the adjoint state variables $\phi^*(\mathbf{x}, t)$ and $\phi_0^*(\mathbf{x})$ depend on the observation points and times but not on the pumping characteristics (the pumping rate and the times when the pump is turned on and off), the adjoint state variables presented in Figures 1 and 2 are applicable to both Cases A and B.

5.2. Head Sensitivities Under Constant Hydraulic Gradient (Case A)

Once we solved for the adjoint state variables and mean heads, we can evaluate the sensitivities. Here we first investigate the differences in head sensitivity $y^{(k,l)}(\mathbf{x})$ between three different solutions for Case A. The first solution only accounts for the element containing $\mathbf{x}$, as shown in (45). As mentioned earlier, in an extreme case where the element size is the same as the domain size, the sensitivity will be zero because of the fact that $u_1(\alpha_m) = 0$ in (45). The second solution is the point-wise sensitivity, which is a limiting case of the first solution normalized by the area of the encompassing element. In the third solution, the correlation of the heterogeneous transmissivity field is taken into account. The comparison is illustrated in Figure 3 as contour maps of the sensitivity of head at observation well $\mathbf{x}_k$ at $t = 500$ days with respect to transmissivity in the entire domain. Visual examination of the figure suggests the general spatial pattern is consistent among three solutions: positive sensitivity in the upgradient (to the left) direction of the observation well and negative in the downgradient direction, indicating that increasing transmissivity in the upgradient direction will likely increase the head at the observation well, while increasing transmissivity in the downgradient direction will decrease the head at the observation well. In addition, it is noted that the patterns in Figures 3a and 3b are nearly identical, except that the latter is much smaller in magnitude. This is due to the fact that the solution in Figure 3a reflects the total effect of exclusive elements of a fixed size (mesh size $100\,\text{m} \times 100\,\text{m} = 10,000\,\text{m}^2$ in area), while the solution in Figure 3b is the head sensitivity with respect to transmissivity at a single point $\mathbf{x}$. In both Figures 3a and 3b cases (uncorrelated fields), the contour lines are not very smooth. The contour lines are significantly smoother in Figure 3c, in which the correlation of the transmissivity field has been considered. The magnitude of the sensitivity in the third solution is much greater than those from the first two solutions. This is expected due to the parameter correlation. In the following discussion, we assume that the parameter fields are correlated.

Figure 4 shows the hydraulic-head sensitivity profile $y^{(k,l)}(\mathbf{x})$ along the central line $\mathbf{x} = (x_1, 2000\,\text{m})^T$. Here the curves for different observation times overlap and the observation time is not relevant because of the time-independent mean head field. It is noted that the head sensitivity is zero at the observation point $\mathbf{x} = \mathbf{x}_k$; i.e., the hydraulic head at the observation point is independent of the transmissivity at the observation point.

The sensitivity $y^{(k,l)}(\mathbf{x})$ for a series of observation points $\mathbf{x}_k = (x_{1k}, x_{2k} = 2000\,\text{m})^T$ for various x_{1k} with respect to $Y(\mathbf{x})$ along the central line $\mathbf{x} = (x_1, 2000\,\text{m})^T$ is illustrated in Figure 5. Typically, the sensitivity profile for

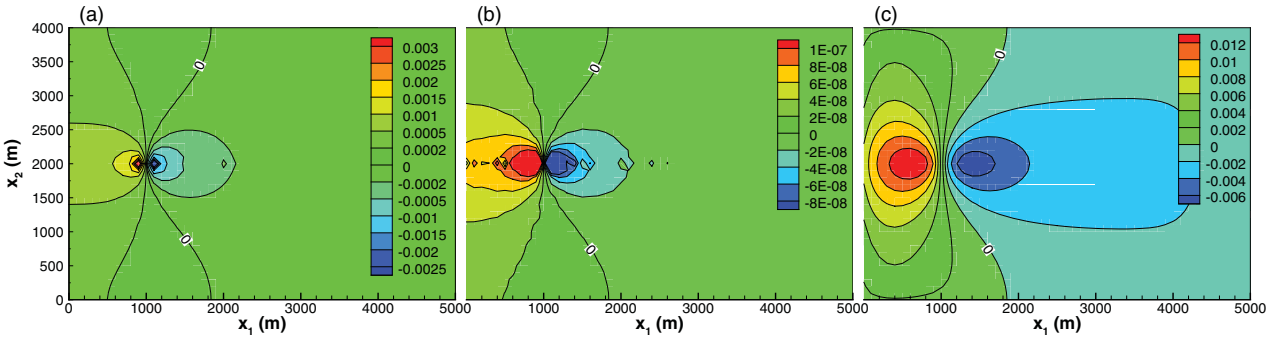

Figure 3. Head sensitivity $\partial h(\mathbf{x}_k, t_l)/\partial Y(\mathbf{x})$ for $\mathbf{x}_k = (1000\,\text{m}, 2000\,\text{m})$ at observation time $t_l = 500$ days, derived from three different approaches assuming: (a) exclusive element containing $\mathbf{x}$, (b) point-wise evaluation, and (c) correlated transmissivity field.

each observation point has a positive peak and a negative peak. The constant-head boundaries have some effect on the magnitude of these peaks. This can be clearly seen from the profile for the observation point at $(200\,\text{m}, 2000\,\text{m})$; without the boundary, the sensitivity at the upgradient boundary (i.e., $x_1 = 0$) would have been larger. It should be pointed out that one should not expect the sensitivity to be zero at these constant-head boundaries unless the observation points are located at these boundaries. As the observation point moves away from the upgradient boundary toward the downgradient boundary, the magnitude of the positive peak decreases while the magnitude of the negative peak increases. Mathematically, one can easily show for this particular case (both $x_2 = x_{2k} = L_2/2$) that the area (i.e., the integral) under each of the curves in this figure is zero.

The locations of the peaks on this profile are approximately symmetric about the observation point and they are related to the correlation length of the transmissivity field, as demonstrated in Figure 6. The figure depicts the sensitivity profile of $y^{(k,l)}(\mathbf{x})$ along the central line $\mathbf{x} = (x_1, 2000\,\text{m})^T$ for observation at $\mathbf{x}_k$ for isotropic transmissivity fields with different correlation lengths $\lambda_{Y,1} = \lambda_{Y,2} = 50\,\text{m}$, 100 m, 200 m, or 250 m. As expected, the transmissivity field with a larger correlation length has larger impact on the head at the observation point (Figure 6). For comparison, the corresponding sensitivity profile is plotted for the case of an uncorrelated field (Figure 6; dashed line) by solving (45) from the integration over the exclusive grid element containing $\mathbf{x}$, where the size of the grid element is 50 m. As expected, the sensitivity profile for an uncorrelated field has the lowest values.

5.3. Transient Head Sensitivities With Pumping (Case B)

So far none of the numerical examples account for the impact of groundwater pumping and the presented sensitivities were for the case of ambient groundwater flow only. Next, we consider a similar case (Case B) in which a well pumping at a constant rate of $20\,\text{m}^3/\text{d}$ is located in the center of the domain, $\mathbf{x}^{(p)} = (2500\,\text{m}, 2000\,\text{m})^T$.

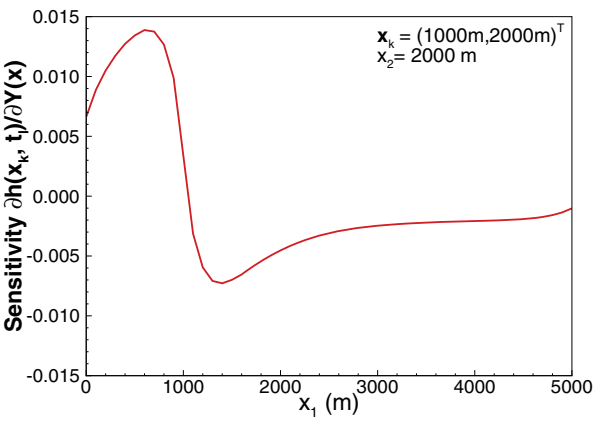

Figure 4. Profile of head sensitivity $\partial h(\mathbf{x}_k, t_l)/\partial Y(\mathbf{x})$ along the central line $\mathbf{x} = (x_1, x_2 = 2000\,\text{m})$ for observation well at $\mathbf{x}_k = (1000\,\text{m}, 2000\,\text{m})$. All curves for different observation time t_l overlap each other for the case of no pumping.

Figure 7 shows snapshots of $y^{(k,l)}(\mathbf{x})$ and $z^{(k,l)}(\mathbf{x})$ for the observation point at $\mathbf{x}_k$ at 100 days. It is important to note that the head at the observation point is predominantly sensitive to the storativity (Figure 7b) within a symmetric area encompassing the pumping and observation wells (e.g., the contour line for $z^{(k,l)}(\mathbf{x}) = 0.0001$ is almost an ellipse, and the wells are near the ellipse focal points). The highest sensitivity is at the well locations. This is not surprising based on existing theory and practical experience. In contrast the head at the observation point is predominantly sensitive to the transmissivity between the

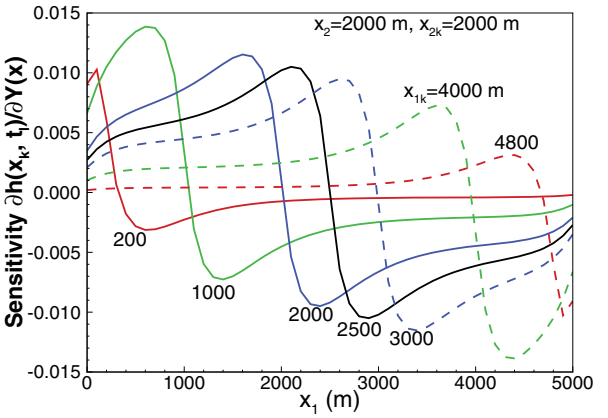

Figure 5. Profiles of head sensitivity $\partial h(\mathbf{x}_k, t_l)/\partial Y(\mathbf{x})$ along the central line $\mathbf{x} = (x_1, x_2 = 2000\,\text{m})$ for different observation locations $\mathbf{x}_k = (x_{1k}, x_{2k} = 2000\,\text{m})$ placed along the central line as well.

two wells and upgradient from the observation well (between the observation well and the constant-head boundary). This observation is also not surprising based on existing theory and practical experience. Note that the spatial pattern of the sensitivity is slightly different from the sensitivity for the unbounded domain, as presented in *Leven and Dietrich* [2006]

5.3.1. The Effect of Observation Times on Head Sensitivities

One of the interesting topics involving head observations is the selection of an optimal sampling frequency or sampling location. It is possible to look for an optimal observation time or location based on sensitivity maps, as shown in Figures 8 and 10 for sensitivities $y^{(k,l)}(\mathbf{x})$ and $z^{(k,l)}(\mathbf{x})$ along the central line $x_2 = 2000$ m as a function of the observation time and location. These maps may shed light on how to select the optimal sample schedule and locations.

Figure 8 depicts the sensitivities of head at $\mathbf{x}_k$ to the transmissivity (Figure 8a) or storativity (Figure 8b) along the central line $\mathbf{x} = (x_1, x_2 = 2000\,\text{m})^T$, for various observation times. It is seen from this figure that the general pattern of this sensitivity is the same for different observation times. This pattern reveals several interesting points. First, the sensitivity is negative in the area between the pumping well and the observation well, indicating that increasing transmissivity in this area will lead to lower head (or greater drawdown) at the observation well. Outside of this area, the sensitivity is positive, which can also be easily explained. In fact, a higher transmissivity beyond the pumping well in the downgradient direction leads to more water coming from that direction. On the other hand, a higher transmissivity in the upgradient direction of the observation well leads to a higher head measurement at the observation well due to the constant head on the upgradient boundary. In addition, the sensitivity changes its sign across the well locations and is zero at both pumping well and observation wells. In other words, transmissivity values at these well locations are not relevant to the head at the observation location. Furthermore, there are two peaks (one positive and one negative) around both pumping and observation wells, and the locations of these peaks move slowly away from the wells with increasing observation time. This suggests that by using transient head data it may be possible to characterize aquifer heterogeneity in different portions of the aquifer near the pumping and observation wells (e.g., between the wells, at early times, and near the wells, at late times).

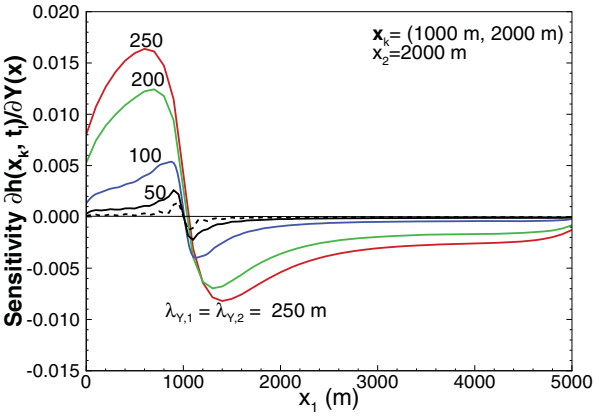

Figure 6. Profiles of head sensitivity $y^{(k,l)}(\mathbf{x}) = \partial h(\mathbf{x}_k, t_l)/\partial Y(\mathbf{x})$ along the central line $\mathbf{x} = (x_1, x_2 = 2000\,m)$ for observation point $\mathbf{x}_k = (1000\,\text{m}, 2000\,\text{m})$ for different correlation lengths of the log transmissivity field. For comparison, the corresponding sensitivity profile is plotted for the case of uncorrelated field using a dashed line (obtained by solving equation (45) from the integration over the exclusive grid element containing $\mathbf{x}$, where the size of the grid element is 50 m).

A similar plot for the sensitivity $z^{(k,l)}(\mathbf{x})$ for the same observation well with various observation times is illustrated in Figure 8b. Unlike the head sensitivity to transmissivity, the sensitivity to storativity is always positive in the entire domain, indicating that an increase of the storativity in any location in the domain will lead to a higher head (or less drawdown) at the observation well because more groundwater is available from storage. The figure shows several important features of the sensitivity pattern.

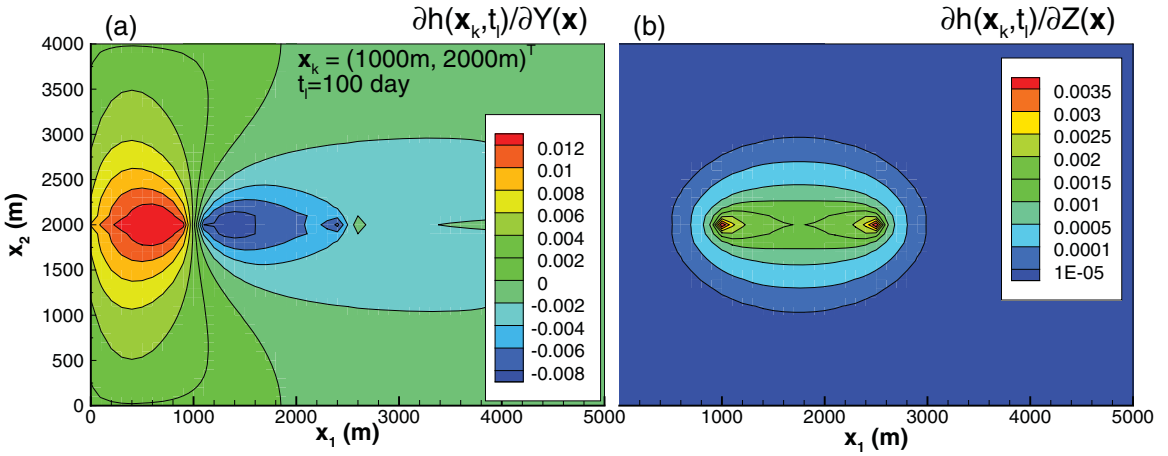

Figure 7. Contour maps of (a) $\partial h(\mathbf{x}_k, t_l)/\partial Y(\mathbf{x})$ and (b) $\partial h(\mathbf{x}_k, t_l)/\partial Z(\mathbf{x})$ for observation well at $\mathbf{x}_k = (1000\,\text{m}, 2000\,\text{m})$ and pumping well at $\mathbf{x}^p = (2500\,\text{m}, 2000\,\text{m})$ at $t_l = 100$ days.

First, the sensitivity has two peaks on the profile, one at the pumping well and the other at observation well. In fact, these two peaks are symmetric in the sense that sensitivity profiles will be the same if one switches the pumping well and the observation locations. This can be shown from (49) for this particular case with one pumping well. Of course, if there is more than one pumping well, such a switch will definitely change the sensitivity profile. The sensitivity in the area between these wells is about half the peak value and outside of this area it decreases sharply.

The change of this sensitivity over observation time is better illustrated in Figure 9, which shows $z^{(k,l)}(\mathbf{x})$ at observation well $\mathbf{x}_k$, as a function of observation time t_l, to storativity at two different locations $\mathbf{x} = (1000\,\text{m}, 2000\,\text{m})$ and $\mathbf{x} = (900\,\text{m}, 2000\,\text{m})$. Although both curves in the figure have the same pattern, i.e., increasing at early time and decreasing at late time, they reach their maximum at different times: 350 days for the solid curve and 400 days for the dashed curve. This may imply that, for given pumping and observation well locations, the best observation time for characterizing storativity at the observation location $(1000\,\text{m}, 2000\,\text{m})$ is 350 days but for characterizing storativity at $(900\,\text{m}, 2000\,\text{m})$ is 400 days. In addition, the maximum sensitivity decreases quickly as the location moves away from the observation well, suggesting that head observations are predominantly sensitive to the storativity at the wells and that the spatial heterogeneity in storativity might be difficult to characterize.

5.3.2. The Effect of Observation Locations on Head Sensitivities

Next, we explore, for a fixed observation time $t_l = 100$ days, the effect of the observation location along the central line through the model domain, as illustrated in Figure 10. Each curve in the figure represents the

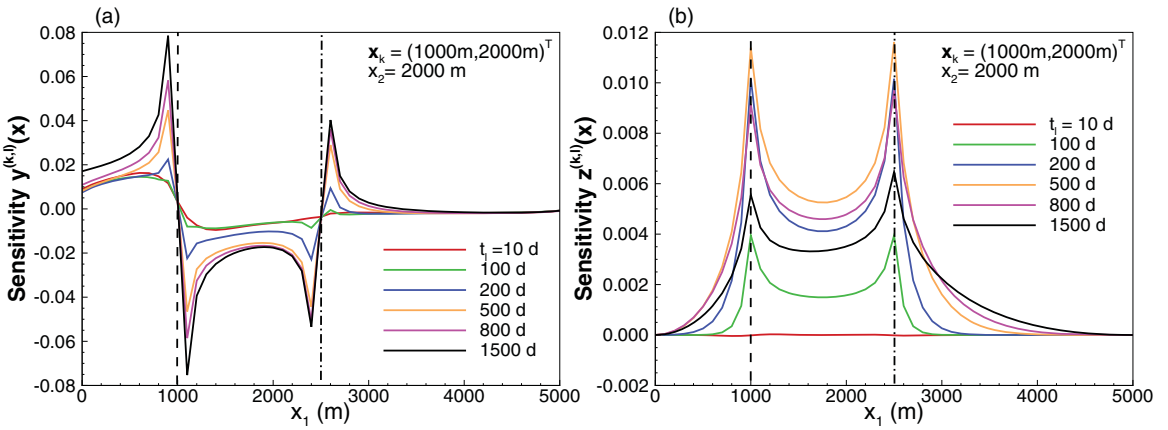

Figure 8. Profiles of head sensitivities (a) $y^{(k,l)}(\mathbf{x}) = \partial h(\mathbf{x}_k, t_l)/\partial Y(\mathbf{x})$ and (b) $z^{(k,l)}(\mathbf{x}) = \partial h(\mathbf{x}_k, t_l)/\partial Z(\mathbf{x})$ along the central line $\mathbf{x} = (x_1, x_2 = 2000\,\text{m})$ for head measurements at different observation times. Here both the pumping and observation wells are located along the line $x_2 = 2000$ m passing through the center of the model domain, with x_1 indicated as a dash-dotted line and a dashed line, respectively.

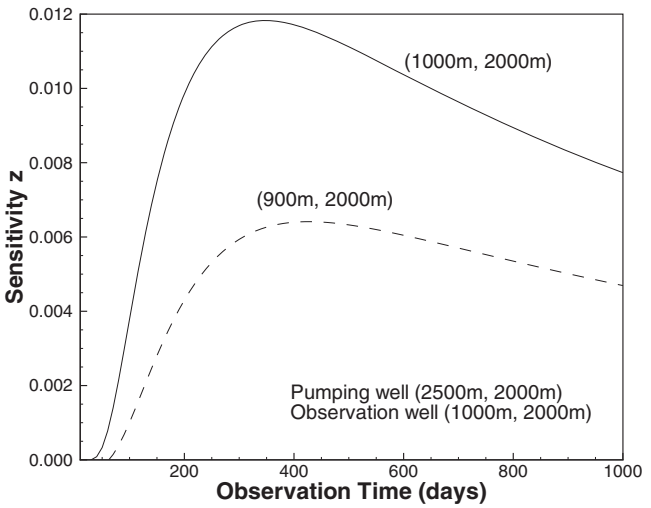

Figure 9. Head sensitivities $z^{(k,l)}(\mathbf{x})=\partial h(\mathbf{x}_k,t_l)/\partial Z(\mathbf{x})$ at $\mathbf{x}_k=(1000\,\mathrm{m},2000\,\mathrm{m})$, as a function of observation time t_l, to storativity at two locations: $\mathbf{x}=(1000\,\mathrm{m},2000\,\mathrm{m})$ and $\mathbf{x}=(900\,\mathrm{m},2000\,\mathrm{m})$. The pumping well is located at $\mathbf{x}^p=(2500\,\mathrm{m},2000\,\mathrm{m})$.

head sensitivity at the observation location $(x_{1k},2000\,\mathrm{m})$, where the value of x_{1k} is labeled on the curve (see Figure 10b). Again, the pumping well is located at the center of the model domain. The general pattens of the sensitivity profiles are as discussed in the last section. We are interested in how these profiles change with the observation location.

Figure 10a shows that, as the observation well location gets closer the pumping well, the sensitivity $y^{(k,l)}(\mathbf{x})$ increases for all points on the profile. As discussed previously, the sensitivity profile includes one positive peak and one negative peak in the vicinity of both pumping and observation wells, and the sensitivity is zero at the well locations. Interestingly, as the observation well aligns with the pumping well, the profile changes significantly to a single spike of 5.5 (the actual peak is not shown in the figure; it has been truncated due to the plotting scale) at the well location, which means that the measuring drawdown at the pumping well provides the most significant amount of information regarding the transmissivity at the pumping well location. This is why single-well pumping tests provide representative information about the transmissivity in the close vicinity of the pumping wells. A similar phenomenon occurs in Figure 10b (semilog plot) for sensitivity $z^{(k,l)}(\mathbf{x})$, where the two-peak profile changes to a single peak when the observation well aligns with the pumping well, which indicates that the single-well pumping test can also be applied to estimate storativity. However, clearly the head's sensitivity to the

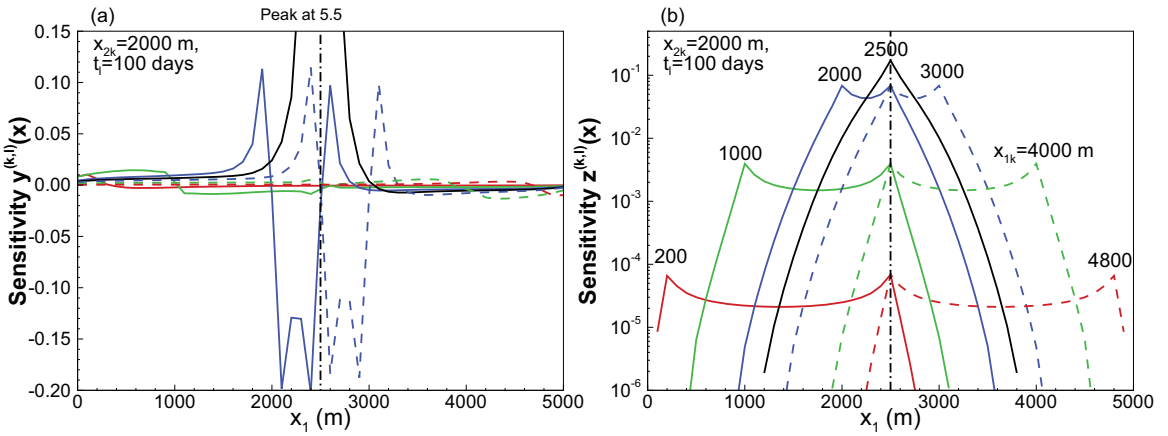

Figure 10. Profiles of head sensitivities (a) $y^{(k,l)}(\mathbf{x})=\partial h(\mathbf{x}_k,t_l)/\partial Y(\mathbf{x})$ and (b) $z^{(k,l)}(\mathbf{x})=\partial h(\mathbf{x}_k,t_l)/\partial Z(\mathbf{x})$ along the central line $\mathbf{x}=(x_1,x_2=2000\,\mathrm{m})$ for observation time $t_l=100$ days at various observation locations $\mathbf{x}_k=(x_{1k},x_{2k}=2000\,\mathrm{m})$ along the central line (the pumping well is located at $x_1=2500\,m$ and the location is marked with a dash-dotted line).

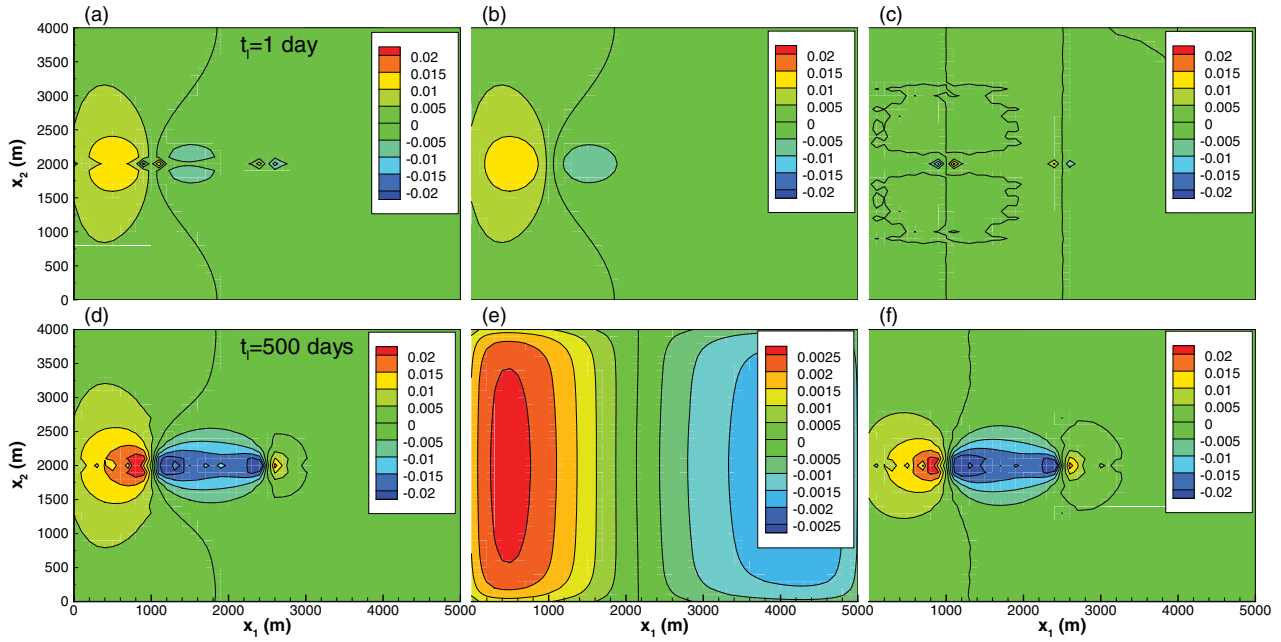

Figure 11. Head sensitivity $\partial h(\mathbf{x}_k, t_l)/\partial Y(\mathbf{x})$, for $\mathbf{x}_k = (1000\,\text{m}, 2000\,\text{m})$ at two observation times $t_l = 1$ day and 500 days. (a and d) The correct sensitivities at these two times; (b and e) contribution from the last term in (17) or (23) or (24); and (c and f) the sensitivities when this additional term is ignored.

storativity is much less than it's sensitivity to the transmissivity; that is one of the reasons the transmissivity is more reliably estimated from single-well pumping tests than the storativity (in addition, storativity estimates are also impacted by wellbore storage and skin effects [*Kabala*, 2001]). In summary, head at the observation location is highly sensitive to storativity at the pumping and observation wells, moderately sensitive to storativity in the area between pumping and observation wells (note: this plot on the log scale).

5.3.3. The Contribution of the Last Term in Equation (17)

Finally, we investigated the contribution from the last term in equation (17) or (23) or (24) for evaluating head sensitivity to log transmissivity. This term accounts for the effect of the initial hydraulic gradient and is ignored in some studies. From (47), it is seen that this term depends on the observation time and it cancels out with the similar term resulting from the first term in (24). If one ignores this term, the sensitivity will depend on the observation time even for the special case where the mean head is time-independent, which is certainly not physical. It is also of interest to evaluate the contribution of this term to the estimated sensitivity field.

Figure 11 provides comparisons for $t_l = 1$ day (Figures 11a–11c) and $t_l = 500$ days (Figures 11d–11f) for Case B. Here Figures 11a and 11d represent the true sensitivity at these two times, Figures 11b and 11e are the contribution of the last term in (17), while Figures 11c and 11f represent the estimated sensitivity if this term is dropped. It is seen that at later times, Figure 11f is quite close to Figure 11d, indicating that one may ignore this term at later times. However, if one is concerned with the early-time head observations, this term should not be ignored, as Figure 11c is significantly different from Figure 11a. If the last term is not applied in sensitivity analyses, the results will be misleadingly suggesting very low head sensitivities to the conductivity at early times.

6. Conclusions

The objective of the paper is to develop a novel analytical methodology based on an adjoint method to compute sensitivities of the hydraulic head to the distributed hydraulic conductivity and storage coefficient in the case of transient groundwater flow in a confined, spatially correlated or uncorrelated, randomly heterogeneous aquifer under ambient and pumping conditions. The methodology is based on an adjoint method and it is applicable to transient groundwater flow in a bounded aquifer pumped at a series of wells,

each of which may have one or more constant-rate pumping periods. The major difference between this study and all previous adjoint-based studies on head (or drawdown) sensitivity is that the spatial correlation of the parameter field has been considered, while in previous studies the parameter field is assumed to be uncorrelated and the integral over the entire problem domain was reduced to an exclusive element (or subdomain) containing the point at which the sensitivity is desired. While the parameter sensitivities with the adjoint method are typically obtained numerically, we present analytical expressions for these sensitivities in the special case of rectangular domains with constant-head and no-flow boundaries. However, it can be extended to three-dimensional problems.

One of advantages of the adjoint method is that the adjoint state variable is independent of the sources/sinks and the actual head or flux values on the boundaries, and therefore the methodology is also applicable to more complicated cases with areal sources/sinks and time-dependent boundary conditions. The effect of areal sources/sinks and boundary conditions on the sensitivities is taken into account through the mean head field, which is applied in evaluating these sensitivities.

The parameter sensitivities with the adjoint method are typically obtained numerically, and the most time-consuming part of the method is solving the adjoint state equations. In our analytical expressions, these sensitivities are represented directly in terms of the problem configuration (the domain size, boundary configuration, pumping well locations, pumping schedule and rates), medium properties (the means and correlation lengths of log transmissivity and log storativity), and observation information (locations and times), and therefore there is no need to solve the adjoint state equations.

The presented framework for estimation of sensitivities of observed hydraulic heads to the aquifer properties is applicable to various types of model analyses such as sensitivity analysis, model inversion, parameter estimation, model selection, uncertainty quantification, data-worth analysis, experimental design, and decision analysis. The framework is particularly relevant to tomographic analyses aimed at the characterization of spatial variability in the aquifer properties. We have presented a series of results obtained for a synthetic problem representing a pumping and an observation well in a rectangular domain with ambient groundwater flow. We have demonstrated the applicability of our methodology to investigate the impact of observation well location and the observation time on the estimates of aquifer properties based on computed spatial and temporal sensitivities.

Appendix A: Functions in (45) and (49) for Uncorrelated Fields

For simplicity in presentation, the following list of functions are defined for (45) and (49) for the case of uncorrelated transmissivity and storativity fields. Equations (A1)–(A5) are related to the mesh element containing the location $\mathbf{x}$ where the sensitivity to transmissivity or storativity at this location is sought. Equations (A6)–(A9) are related to observation time and the pumping period, and therefore they are valid for both uncorrelated and correlated fields. Some important features of these functions include: (a) $F_1^{\pm}$ and $F_2^{\pm}$ are symmetric in terms of their arguments, (b) $I_T^{(i)}$ and $I_S^{(i)}$ are symmetric in terms of their indices m, m_1, n, and n_1, and (c) u_1 is zero if $x_1 = L_1/2$ and the element size in the x_1 direction is L_1.

$$u_1(\alpha_m) = \frac{2}{\alpha_m}\cos(\alpha_m x_1)\sin(\alpha_m \Delta x_1/2) \tag{A1}$$

$$u_2(\beta_n) = \begin{cases} \dfrac{2}{\beta_n}\cos(\beta_n x_2)\sin(\beta_n \Delta x_2/2) & \text{if } n > 0 \\ \Delta x_2 & \text{if } n = 0 \end{cases} \tag{A2}$$

$$F_1^{\pm}(\alpha_m, \alpha_{m_1}) = \begin{cases} \dfrac{\cos[(\alpha_m - \alpha_{m_1})x_1]\sin[(\alpha_m - \alpha_{m_1})\Delta x_1/2]}{\alpha_m - \alpha_{m_1}} \\ \pm \dfrac{\cos[(\alpha_m + \alpha_{m_1})x_1]\sin[(\alpha_m + \alpha_{m_1})\Delta x_1/2]}{\alpha_m + \alpha_{m_1}} & \text{if } m \neq m_1 \\ \dfrac{\Delta x_1}{2} \pm \dfrac{\cos(2\alpha_m x_1)\sin(\alpha_m \Delta x_1)}{2\alpha_m} & \text{if } m = m_1 \end{cases} \tag{A3}$$

$$F_2^+(\beta_n,\beta_{n_1})=\begin{cases}\dfrac{\cos[(\beta_n-\beta_{n_1})x_2]\sin[(\beta_n-\beta_{n_1})\Delta x_2/2]}{\beta_n-\beta_{n_1}} & \\ +\dfrac{\cos[(\beta_n+\beta_{n_1})x_2]\sin[(\beta_n+\beta_{n_1})\Delta x_2/2]}{\beta_n+\beta_{n_1}} & \text{if } n,n_1\neq 0, n\neq n_1\\ \dfrac{\Delta x_2}{2}+\dfrac{\cos(2\beta_n x_2)\sin(\beta_n\Delta x_2)}{2\beta_n} & \text{if } n,n_1\neq 0, n=n_1\\ \dfrac{2}{\beta_n}\cos(\beta_n x_2)\sin(\beta_n\Delta x_2/2) & \text{if } n_1=0, n\neq 0\\ \dfrac{2}{\beta_{n_1}}\cos(\beta_{n_1}x_2)\sin(\beta_{n_1}\Delta x_2/2) & \text{if } n_1\neq 0, n=0\\ \Delta x_2 & \text{if } n_1=0, n=0\end{cases} \tag{A4}$$

$$F_2^-(\beta_n,\beta_{n_1})=\begin{cases}\dfrac{\cos[(\beta_n-\beta_{n_1})x_2]\sin[(\beta_n-\beta_{n_1})\Delta x_2/2]}{\beta_n-\beta_{n_1}} & \\ -\dfrac{\cos[(\beta_n+\beta_{n_1})x_2]\sin[(\beta_n+\beta_{n_1})\Delta x_2/2]}{\beta_n+\beta_{n_1}} & \text{if } n,n_1\neq 0, n\neq n_1\\ \dfrac{\Delta x_2}{2}-\dfrac{\cos(2\beta_n x_2)\sin(\beta_n\Delta x_2)}{2\beta_n} & \text{if } n,n_1\neq 0, n=n_1\\ 0 & \text{if } nn_1=0\end{cases} \tag{A5}$$

The definition of $I_T^{(i)}$ depends on the the value of $\omega_{m_1n_1}^2-\omega_{mn}^2$. If $\omega_{m_1n_1}^2\neq\omega_{mn}^2$:

$$I_T^{(i)}=\begin{cases}0 & \text{if } t_l<t_i^s\\ \dfrac{1-e^{\frac{\bar{T}}{S}\omega_{m_1n_1}^2(t_i^s-t_l)}}{\omega_{m_1n_1}^2}-\dfrac{e^{\frac{\bar{T}}{S}\omega_{mn}^2(t_i^s-t_l)}-e^{\frac{\bar{T}}{S}\omega_{m_1n_1}^2(t_i^s-t_l)}}{\omega_{m_1n_1}^2-\omega_{mn}^2} & \text{if } t_i^s<t_l\le t_i^e\\ \dfrac{e^{\frac{\bar{T}}{S}\omega_{m_1n_1}^2(t_i^e-t_l)}-e^{\frac{\bar{T}}{S}\omega_{m_1n_1}^2(t_i^s-t_l)}}{\omega_{m_1n_1}^2} & \\ -\dfrac{e^{\frac{\bar{T}}{S}\omega_{mn}^2(t_i^s-t_l)}-e^{\frac{\bar{T}}{S}\omega_{m_1n_1}^2(t_i^s-t_l)}-e^{\frac{\bar{T}}{S}\omega_{mn}^2(t_i^e-t_l)}+e^{\frac{\bar{T}}{S}\omega_{m_1n_1}^2(t_i^e-t_l)}}{\omega_{m_1n_1}^2-\omega_{mn}^2} & \text{if } t_l>t_i^e,\end{cases} \tag{A6}$$

otherwise,

$$I_T^{(i)}=\begin{cases}0 & \text{if } t_l<t_i^s\\ \dfrac{1-e^{\frac{\bar{T}}{S}\omega_{m_1n_1}^2(t_i^s-t_l)}}{\omega_{m_1n_1}^2}-\dfrac{\bar{T}}{S}(t_l-t_i^s)e^{\frac{\bar{T}}{S}\omega_{mn}^2(t_i^s-t_l)} & \text{if } t_i^s<t_l\le t_i^e\\ \dfrac{e^{\frac{\bar{T}}{S}\omega_{mn}^2(t_i^e-t_l)}-e^{\frac{\bar{T}}{S}\omega_{mn}^2(t_i^s-t_l)}}{\omega_{mn}^2} & \\ -\dfrac{\bar{T}}{S}(t_l-t_i^s)e^{\frac{\bar{T}}{S}\omega_{mn}^2(t_i^s-t_l)}+\dfrac{\bar{T}}{S}(t_l-t_i^e)e^{\frac{\bar{T}}{S}\omega_{mn}^2(t_i^e-t_l)} & \text{if } t_l>t_i^e\end{cases}. \tag{A7}$$

Similarly,

$$I_S^{(i)}=\begin{cases}0 & \text{if } t_l<t_i^s\\ \dfrac{e^{\frac{\bar{T}}{S}\omega_{mn}^2(t_i^s-t_l)}-e^{\frac{\bar{T}}{S}\omega_{m_1n_1}^2(t_i^s-t_l)}}{\omega_{m_1n_1}^2-\omega_{mn}^2} & \text{if } t_i^s<t_l\le t_i^e\\ \dfrac{e^{\frac{\bar{T}}{S}\omega_{mn}^2(t_i^s-t_l)}-e^{\frac{\bar{T}}{S}\omega_{m_1n_1}^2(t_i^s-t_l)}-e^{\frac{\bar{T}}{S}\omega_{mn}^2(t_i^e-t_l)}+e^{\frac{\bar{T}}{S}\omega_{m_1n_1}^2(t_i^e-t_l)}}{\omega_{m_1n_1}^2-\omega_{mn}^2} & \text{if } t_l>t_i^e\end{cases}, \tag{A8}$$

for $\omega_{mn}^2\neq\omega_{m_1n_1}^2$, and

$$I_S^{(i)} = \begin{cases} 0 & \text{if } t_l < t_i^s \\ \frac{\bar{T}}{\bar{S}}(t_l - t_i^s)e^{\frac{\bar{T}}{\bar{S}}\omega_{mn}^2(t_i^s - t_l)} & \text{if } t_i^s < t_l \le t_i^e \\ \frac{\bar{T}}{\bar{S}}\left[(t_l - t_i^s)e^{\frac{\bar{T}}{\bar{S}}\omega_{mn}^2(t_i^s - t_l)} - (t_l - t_i^e)e^{\frac{\bar{T}}{\bar{S}}\omega_{mn}^2(t_i^e - t_l)}\right] & \text{if } t_l > t_i^e \end{cases}, \tag{A9}$$

otherwise. Note that (A7) and (A9) can be derived by taking the limit of (A6) and (A8), respectively, as $\omega_{mn}^2 \to \omega_{m_1 n_1}^2$.

Appendix B: Functions in (45) and (49) for Correlated Fields

If the transmissivity is spatially correlated, (45) is still valid, but function definitions for u_1, u_2, $F_1^{\pm}$, and $F_2^{\pm}$ are slightly different:

$$u_1(\alpha_m) = \frac{\lambda_{Y,1}}{\alpha_m^2\lambda_{Y,1}^2 + 1}\left[2\cos(\alpha_m x_1) - \left(e^{-\frac{x_1}{\lambda_{Y,1}}} + (-1)^m e^{-\frac{L_1 - x_1}{\lambda_{Y,1}}}\right)\right] \tag{B1}$$

$$u_2(\beta_n) = \frac{\lambda_{Y,2}}{\beta_n^2\lambda_{Y,2}^2 + 1}\left[2\cos(\beta_n x_2) - \left(e^{-\frac{x_2}{\lambda_{Y,2}}} + (-1)^n e^{-\frac{L_2 - x_2}{\lambda_{Y,2}}}\right)\right] \tag{B2}$$

$$\begin{aligned} F_1^{\pm}(\alpha_m, \alpha_{m_1}) = {} & \frac{\lambda_{Y,1}}{2}\left[\frac{2\cos[(\alpha_m - \alpha_{m_1})x_1]}{A^-} \pm \frac{2\cos[(\alpha_m + \alpha_{m_1})x_1]}{A^+}\right] \\ & + \frac{\lambda_{Y,1}}{2}\frac{A^+ \pm A^-}{A^+ A^-}\left[e^{-\frac{x_1}{\lambda_{Y,1}}} + (-1)^{m+m_1} e^{-\frac{L_1 - x_1}{\lambda_{Y,1}}}\right] \end{aligned} \tag{B3}$$

$$\begin{aligned} F_2^{\pm}(\beta_n, \beta_{n_1}) = {} & \frac{\lambda_{Y,2}}{2}\left[\frac{2\cos[(\beta_n - \beta_{n_1})x_2]}{B^-} \pm \frac{2\cos[(\beta_n + \beta_{n_1})x_2]}{B^+}\right] \\ & + \frac{\lambda_{Y,2}}{2}\frac{B^+ \pm B^-}{B^+ B^-}\left[e^{-\frac{x_2}{\lambda_{Y,2}}} + (-1)^{n+n_1} e^{-\frac{L_2 - x_2}{\lambda_{Y,2}}}\right] \end{aligned} \tag{B4}$$

where $\lambda_{Y,1}$ and $\lambda_{Y,2}$ are the correlation lengths of the log transmissivity in the x_1 and x_2 directions, respectively, and $A^{\pm} = (\alpha_m \pm \alpha_{m_1})^2\lambda_{Y,1}^2 + 1$, $B^{\pm} = (\beta_n \pm \beta_{n_1})^2\lambda_{Y,2}^2 + 1$. Similarly, functions F_1^- and F_2^+ for (49) can be derived by replacing $\lambda_{Y,1}$ and $\lambda_{Y,2}$ in (B3) and (B4) by $\lambda_{Z,1}$ and $\lambda_{Z,2}$, respectively.

Acknowledgments
This research was funded by the Environmental Programs Directorate of the Los Alamos National Laboratory. The data to support this paper are available, and can be obtained by contacting Zhiming Lu at zhiming@lanl.gov. The authors wish to thank the associated editor and three anonymous reviewers for comments that substantially improved the manuscript. The authors are grateful to Daniel O'Malley for his thorough review on the paper.

References

Becker, L., and W. W.-G. Yeh (1972), Identification of parameters in unsteady open channel flows, *Water Resour. Res.*, *8*(4), 956–965.
Binning, P., and M. A. Celia (1996), A finite volume eulerian-lagrangian localized adjoint method for solution of the contaminant transport equations in two-dimensional multiphase flow systems, *Water Resour. Res.*, *32*(1), 103–114.
Butler, J. J., and W. Liu (1993), Pumping tests in nonuniform aquifers: The radially asymmetric case, *Water Resour. Res.*, *29*(2), 259–269.
Butler, J. J., and W. Z. Liu (1991), Pumping tests in non-uniform aquifersthe linear strip case, *J. Hydrol.*, *128*(1), 69–99.
Carrera, J., and A. Medina (1994), An improved form of adjoint-state equations for transient problems, in *X International Conference on Computational Methods in Water Resources*, edited by A. Peters, et al., vol. 1, 199 pp., Kluwer Academic Publishers, Dordrecht, Netherlands.
Carter, R., L. Kemp Jr., A. Pierce, and D. Williams (1974), Performance matching with constraints, *Soc. Pet. Eng. J.*, *14*(02), 187–196.
Fu, J., H. A. Tchelepi, and J. Caers (2010), A multiscale adjoint method to compute sensitivity coefficients for flow in heterogeneous porous media, *Adv. Water Resour.*, *33*(6), 698–709.
Hughson, D. L., and T.-C. J. Yeh (1998), A geostatistically based inverse model for three-dimensional variably saturated flow, *Stochastic Hydrol. Hydraul.*, *12*(5), 285–298.
Jacquard, P., et al. (1965), Permeability distribution from field pressure data, *Soc. Pet. Eng. J.*, *5*(04), 281–294.
Kabala, Z. (2001), Sensitivity analysis of a pumping test on a well with wellbore storage and skin, *Adv. Water Resour.*, *24*(5), 483–504.
Larbkich, W., R. Neupauer, D. Colvin, J. Bauer, and J. Herman (2014), Adjoint modeling of contaminant fate and transport in riverbank filtration systems, in *World Environmental and Water Resources Congress 2014*, edited by W. C. Huber, pp. 235–242, Am. Soc. of Civ. Eng., Va.
Leven, C., and P. Dietrich (2006), What information can we get from pumping tests?-comparing pumping test configurations using sensitivity coefficients, *J. Hydrol.*, *319*(1), 199–215.
Li, B., and T.-C. J. Yeh (1998), Sensitivity and moment analyses of head in variably saturated regimes, *Adv. Water Resour.*, *21*(6), 477–485.
Li, B., and T.-C. J. Yeh (1999), Cokriging estimation of the conductivity field under variably saturated flow conditions, *Water Resour. Res.*, *35*(12), 3663–3674.
Lu, A., C. Wang, and W.-G. Yeh (1988), Adjoint-state and sensitivity coefficient calculation in multilayer aquifer system, *Dev. Water Sci.*, *36*, 377–384.

Lu, Z., and B. A. Robinson (2006), Parameter identification using the level set method, *Geophys. Res. Lett.*, *33*, L06404, doi:10.1029/2005GL025541.
Lu, Z., and D. Zhang (2003), On stochastic study of well capture zones in bounded, randomly heterogeneous media, *Water Resour. Res.*, *39*(4), 1100, doi:10.1029/2002WR001633.
Lu, Z., and D. Zhang (2005), Analytical solutions to statistical moments for transient flow in two-dimensional, bounded, randomly heterogeneous media, *Water Resour. Res.*, *41*, W01016, doi:10.1029/2004WR003389.
Mao, D., T.-C. J. Yeh, L. Wan, J.-C. Wen, W. Lu, C.-H. Lee, and K.-C. Hsu (2013a), Joint interpretation of sequential pumping tests in unconfined aquifers, *Water Resour. Res.*, *49*, 1782–1796, doi:10.1002/wrcr.20129.
Mao, D., T.-C. J. Yeh, L. Wan, C.-H. Lee, K.-C. Hsu, J.-C. Wen, and W. Lu (2013b), Cross-correlation analysis and information content of observed heads during pumping in unconfined aquifers, *Water Resour. Res.*, *49*, 713–731, doi:10.1002/wrcr.20066.
Mazzilli, N., V. Guinot, and H. Jourde (2010), Sensitivity analysis of two-dimensional steady-state aquifer flow equations. implications for groundwater flow model calibration and validation, *Adv. Water Resour.*, *33*(8), 905–922.
McElwee, C. D., and M. A. Yukler (1978), Sensitivity of groundwater models with respect to variations in transmissivity and storage, *Water Resour. Res.*, *14*(3), 451–459.
Michalak, A. M., and P. K. Kitanidis (2004), Estimation of historical groundwater contaminant distribution using the adjoint state method applied to geostatistical inverse modeling, *Water Resour. Res.*, *40*, W08302, doi:10.1029/2004WR003214.
Neuman, S. P. (1980), A statistical approach to the inverse problem of aquifer hydrology: 3. improved solution method and added perspective, *Water Resour. Res.*, *16*(2), 331–346.
Neupauer, R., and M. Cronin (2010), Adjoint model for the selection of groundwater well locations to minimize stream depletion, in *Congress: World Environmental and Water Resources Congress*, *Challenge of Changes*, edited by R. N. Palmer, pp. 6–10, Am. Soc. of Civ. Eng., Providence., Va.
Neupauer, R. M., and J. L. Wilson (1999), Adjoint method for obtaining backward-in-time location and travel time probabilities of a conservative groundwater contaminant, *Water Resour. Res.*, *35*(11), 3389–3398.
Neupauer, R. M., and J. L. Wilson (2001), Adjoint-derived location and travel time probabilities for a multidimensional groundwater system, *Water Resour. Res.*, *37*(6), 1657–1668.
Özişik, M. N. (1989), *Boundary Value Problems of Heat Conduction*, Courier Corp., Dover Publications, Inc, N. Y.
Piasecki, M., and N. D. Katopodes (1997), Control of contaminant releases in rivers. I: Adjoint sensitivity analysis, *J. Hydraul. Eng.*, *123*(6), 486–492.
Ramasomanana, F., A. Younes, and M. Fahs (2012), Modeling 2d multispecies reactive transport in saturated/unsaturated porous media with the Eulerian–Lagrangian localized adjoint method, *Water Air Soil Pollut.*, *223*(4), 1801–1813.
Saltelli, A., K. Chan, and E. M. Scott (Eds.) (2000), *Sensitivity Analysis*, vol. 134, John Wiley, N. Y.
Sun, N.-Z., and W. W.-G. Yeh (1985), Identification of parameter structure in groundwater inverse problem, *Water Resour. Res.*, *21*(6), 869–883.
Sun, N.-Z., and W. W.-G. Yeh (1992), A stochastic inverse solution for transient groundwater flow: Parameter identification and reliability analysis, *Water Resour. Res.*, *28*(12), 3269–3280.
Sun, R., T.-C. J. Yeh, D. Mao, M. Jin, W. Lu, and Y. Hao (2013), A temporal sampling strategy for hydraulic tomography analysis, *Water Resour. Res.*, *49*, 3881–3896, doi:10.1002/wrcr.20337.
Sykes, J., J. Wilson, and R. Andrews (1985), Sensitivity analysis for steady state groundwater flow using adjoint operators, *Water Resour. Res.*, *21*(3), 359–371.
Yeh, W. W.-G. (1986), Review of parameter identification procedures in groundwater hydrology: The inverse problem, *Water Resour. Res.*, *22*(2), 95–108.
Zhu, J., and T.-C. J. Yeh (2005), Characterization of aquifer heterogeneity using transient hydraulic tomography, *Water Resour. Res.*, *41*, W07028, doi:10.1029/2004WR003790.